CHALMERS

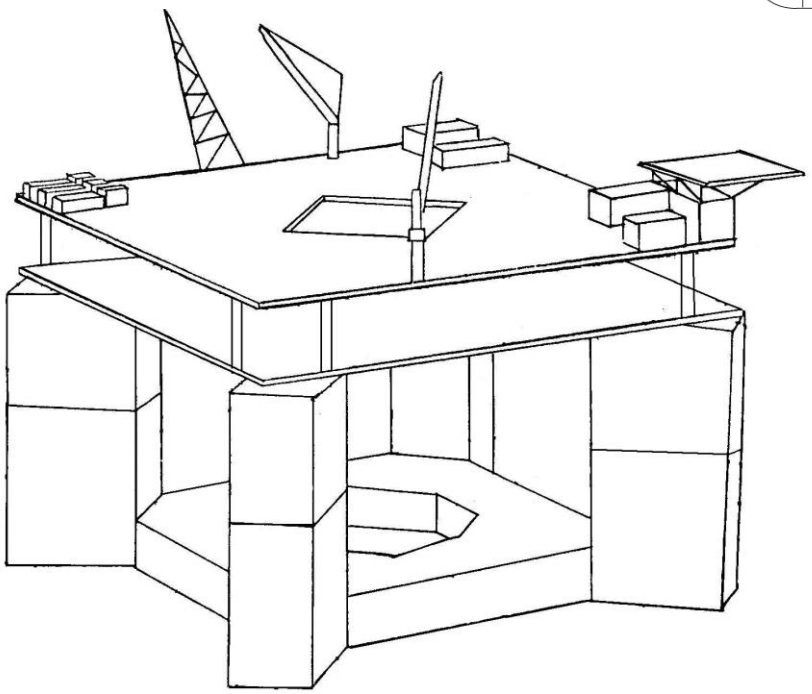

Optimization of a Floating Platform Design

Implementation in the design tool HYDA

Master's Thesis in the International Master's Programme Naval Architecture and Ocean Engineering

HAO CHEN & MD. MEZBAH UDDIN

Department of Shipping and Marine Technology
Division of Marine Design, Research Group Marine Structures
CHALMERS UNIVERSITY OF TECHNOLOGY
Göteborg, Sweden 2013

Master's thesis 2013:X-13/297

MASTER'S THESIS IN THE INTERNATIONAL MASTER'S PROGRAMME IN NAVAL ARCHITECTURE AND OCEAN ENGINEERING

Optimization of a Floating Platform DesignDesign

Implementation in the design tool HYDA

HAO CHEN & MD. MEZBAH UDDIN

Department of Shipping and Marine Technology
Division of Marine Design
Research Group Marine Structures
CHALMERS UNIVERSITY OF TECHNOLOGY

Göteborg, Sweden 2013

Optimization of a Floating Platform DesignDesign
Implementation in the design tool HYDA
HAO CHEN & MD. MEZBAH UDDIN

Master's Thesis 2013:X-13/297
ISSN 1652-8557
Department of Shipping and Marine Technology
Division of Marine Design
Research Group Marine Structures
Chalmers University of Technology
SE-412 96 Göteborg
Sweden
Telephone: + 46 (0)31-772 1000

Chalmers Reproservice / Department of Shipping and Marine Technology
Göteborg, Sweden 2013

Optimization of a Floating Platform Design
Implementation in the design tool HYDA
Master's Thesis in the International Master's Programme in Naval Architecture and Ocean Engineering

HAO CHEN & MD. MEZBAH UDDIN
Department of Shipping and Marine Technology
Division of Marine Design
Research Group Marine Structures
Chalmers University of Technology

ABSTRACT

The design tool HYDA is a FORTRAN program developed at GVA with the purpose of aiding in the design and optimization of floating platforms. In this project a couple of sub-routines that are considered to be of particular interest in HYDA are refined. The considered sub-routines estimate mass budget, wind force, current force, mooring stiffness and static offset. The estimated mass budget is interpolated from two reference models; superstructure and area of facilities on deck are accounted for wind force scaling. For mooring systems, the mean drift force is calculated and included in the sub-routine responsible for calculating static offset and line tension. Moreover, motion responses of three different platforms are evaluated and optimization of the non-conventional unit is assessed using HYDA. The results before and after optimization are listed and compared in this report. From the comparison it can be concluded that the width of the platform after optimization is significantly reduced while the eigenperiod increases. Both of the non-conventional units before and after optimization give a good result in heave motion, which is considerably reduced compared to a conventional unit.

Key words: floating platform, hydrodynamics, optimization,

Contents

Preface

This thesis is a part of the requirements for the master's degree in Naval Architecture and Ocean Engineering at Chalmers University of Technology, Göteborg, and has been carried out at the Division of Marine Design, Department of Shipping and Marine Technology, Chalmers University of Technology between January and June of 2013. We really appreciate many people who have given us a lot of help.

We would like to acknowledge and thank our supervisor Göran Johansson, Carl-Erik Janson and Professor Jonas Ringsberg for sharing their knowledge and experience and providing guidance to us. It has been impossible to implement the project without their help.

Moreover, we would like to thank all the staff of the Hydrodynamic Department in GVA.

Göteborg, June 2013

Hao Chen and Md. Mezbah Uddin

Notations

L_c	Column side length [m]
R	Riser mass [tonnes]
D_{ag}	Draught air gap [m]
H_p	Pontoon height [m]
L_p	Length over column [m]
W_p	Width over column [m]
R_p	Pontoon height ratio
SAG	Static air gap [m]
s	Coefficient to control the slope of the function
T	Topside mass [tonnes]
T_1	Topside mass of the first reference model [tonnes]
T_2	Topside mass of the second reference model [tonnes]
D	Draught [m]
D_1	Draught of first reference model [m]
D_2	Draught of Second reference model [m]
V_a	Volume of pontoon bow/stern/starboard/port side [m^3]
V_{a1}	Volume of pontoon bow/stern/starboard/port side of first reference model [m^3]
V_{a2}	Volume of pontoon bow/stern/starboard/port side of second reference model [m^3]
V_c	Volume of each column [m^3]
V_{c1}	Volume of each column of first reference model [m^3]
V_{c2}	Volume of each column of second reference model [m^3]
E	Equipment mass [tonnes]
E_1	Equipment mass of the first reference model [tonnes]
E_2	Equipment mass of the first reference model [tonnes]
E_{ul}	Upper limit of equipment mass [tonnes]
F	Fuel oil mass [tonnes]
F_1	Fuel oil mass of first reference model [tonnes]
F_2	Fuel oil mass of second reference model [tonnes]
F_{ul}	Upper limit of fuel oil mass [tonnes]
P	Portable water mass [tonnes]
P_1	Portable water mass of first reference model [tonnes]
P_2	Portable water mass of second reference model [tonnes]
P_{ul}	Upper limit of portable water mass [tonnes]
B	Mass of each bow/each stern [tonnes]
B_1	Mass of each bow/each stern of first reference model [tonnes]
B_2	Mass of each bow/each stern of second reference model [tonnes]
B_{ul}	Upper limit of each bow/each stern mass [tonnes]
M	Mass of pontoon bow/stern/starboard/port side [tonnes]

M_1 Mass of pontoon bow/stern/starboard/port side of first reference model [tonnes]

M_2 Mass of pontoon bow/stern/starboard/port side of second reference model [tonnes]

M_{ul} Upper limit of pontoon bow/stern/starboard/port side mass [tonnes]

C Mass of each column [tonnes]

C_1 Mass of each column of first reference model [tonnes]

C_2 Mass of each column of second reference model [tonnes]

C_{ul} Upper limit of each column mass [tonnes]

I Deck box mass [tonnes]

I_1 Deck box mass of first reference model [tonnes]

I_2 Deck box mass of second reference model [tonnes]

I_{ul} Upper limit of deck box mass [tonnes]

J Deck house mass [tonnes]

J_1 Deck house mass of first reference model [tonnes]

J_2 Deck house mass of second reference model [tonnes]

J_{ul} Upper limit of deck house mass [tonnes]

K Equipment in hull mass [tonnes]

K_1 Equipment in hull mass of the first reference model [tonnes]

K_2 Equipment in hull mass of the second reference model [tonnes]

K_{ul} Upper limit of equipment in hull mass [tonnes]

A_f Above water front area [m^2]

A_{f1} Above water front area of first reference model [m^2]

A_{f2} Above water front area of second reference model [m^2]

A_s Above water side area [m^2]

A_{s1} Above water side area of first reference model [m^2]

A_{s2} Above water side area of second reference model [m^2]

H_{su} Head wind force coefficient for surge response [kNs^2/m^2]

H_p Head wind force coefficient for pitch response [kNs^2/m]

H_{su1} Head wind force coefficient for surge response of first reference model [kNs^2/m^2]

H_{su2} Head wind force coefficient for surge response of second reference model [kNs^2/m^2]

H_{sul} Upper limit of head wind force coefficient for surge response [kNs^2/m^2]

H_{sw1} Head wind force coefficient for sway response of first reference model [kNs^2/m^2]

H_{sw2} Head wind force coefficient for sway response of second reference model [kNs^2/m^2]

H_{swul} Upper limit of head wind force coefficient for sway response [kNs^2/m^2]

Q_s Quarter wind force coefficient for surge response [kNs^2/m^2]

Q_p Quarter wind force coefficient for pitch response [kNs^2/m]

Q_{sw} Quarter wind force coefficient for sway response [kNs^2/m^2]

Q_r Quarter wind force coefficient for roll response [kNs^2/m]

Q_{s1} Quarter wind force coefficient for surge response of first reference model [kNs^2/m^2]

Q_{s2} Quarter wind force coefficient for surge response of second reference model [kNs^2/m^2]

Q_{sul} Upper limit of quarter wind force coefficient for surge response [kNs^2/m^2]

Q_{sw1} Quarter wind force coefficient for sway response of first reference model [kNs^2/m^2]

Q_{sw2} Quarter wind force coefficient for sway response of second reference model [kNs^2/m^2]

Q_{swul} Upper limit of quarter wind force coefficient for sway response [kNs^2/m^2]

B_{sw} Beam wind force coefficient for sway response [kNs^2/m^2]

B_r Beam wind force coefficient for roll response [kNs^2/m]

1 Introduction

1.1 Background

Knowledge about the environmental load and motion of offshore structures is of importance both in design and operation. The induced motion response can have a significant impact on offshore structures. Heave motion is a limiting factor for drilling operations since the vertical motion of risers has to be compensated and there are limits to how much the motion can be compensated. Similarly, on a production unit the heave motion impacts on the riser design. Rolling, pitching and accelerations may represent limiting factors for the operation of process equipment on board.

Generally speaking, offshore platforms can be divided into fixed structures and floating platforms. Jack-up and gravity-based structures are typical fixed offshore structures which penetrate the sea floor. Figure 1.1 shows some examples of these.

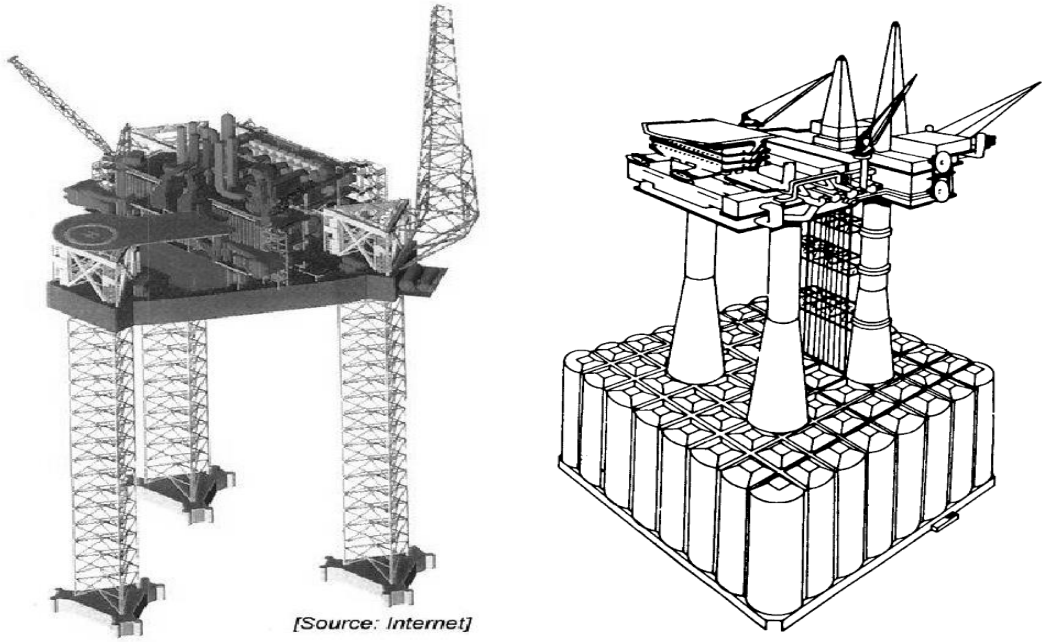

Figure 1.1 Example of a jack- up (left) and gravity- based structure (right)

Semi-submersibles and spar platforms are typical floating platforms and may oscillate in the sea. The tension leg platform is restrained vertically by tethers. Examples of these can be found in Figure 1.2.

In this thesis project, environment load and induced motion responses on offshore floating platforms, especially semi-submersibles, are the most important topic. The theoretical background is adopted from Faltinsen (1993) and Journee (2001).

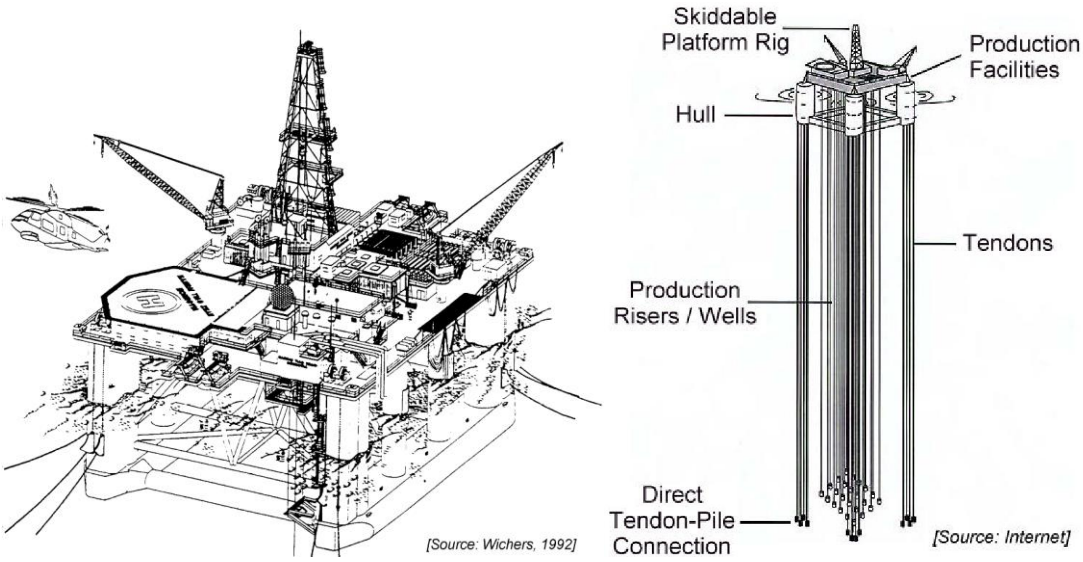

Figure 1.2 Example of semi-submersible (left) and tension leg platform (right)

1.2 Objective

The main objective of this thesis project can be clarified as being in two parts: the optimization of a non-conventional unit and the refinement of particular subroutines the in design tool HYDA. Chapters 7-11 are related to the modification of sub-routines in HYDA, while Chapters 5, 6 and 12 deal with the topic of optimization of non-conventional units.

The design tool HYDA is developed at GVA Consultant AB with the purpose of analysing the motion property of offshore platforms. Several commercial and in-house software are combined in HYDA to perform a state-of-the-art analysis. The detailed analysis procedure is introduced in Chapter 2 and in this thesis project, sub-routines related to mass budget calculation, wind force calculation, current force calculation, mooring stiffness and static offset will be investigated and modified.

The non-conventional unit originates from an American patent (see G. Bergman (1978)). This unit is introduced due to its great performance in heave response. In this thesis, the optimization of the non-conventional unit will be assessed in order to achieve a better performance in motion response, especially heave motion.

2 The Design Tool HYDA

2.1 Existing design tool

HYDA is a FORTRAN program developed at GVA with the purpose of aiding in the design of floating platforms. Depending on the input specified by the users, different sub-routines are called by HYDA either in a sequence or in an iterative fashion.

The input data is stored in the input file *HYDA.INP*, which will be called by HYDA when the program starts to run. The input data is divided into four categories:

1. Primary input, which includes environmental conditions and predefined topside and riser mass.

2. Secondary input, which includes geometric dimensions of the platform.

3. Tertiary input, which includes mesh size of the panel model, optimization option, etc.

4. Target values for the optimization process, which include target heel, target heave, target ballast, etc.

The default input parameters result in the generation of a GENIE panel model and a PREFEM slender-element model of the MORISON type. Examples of a panel model and slender element model are shown in Figure 2.1.

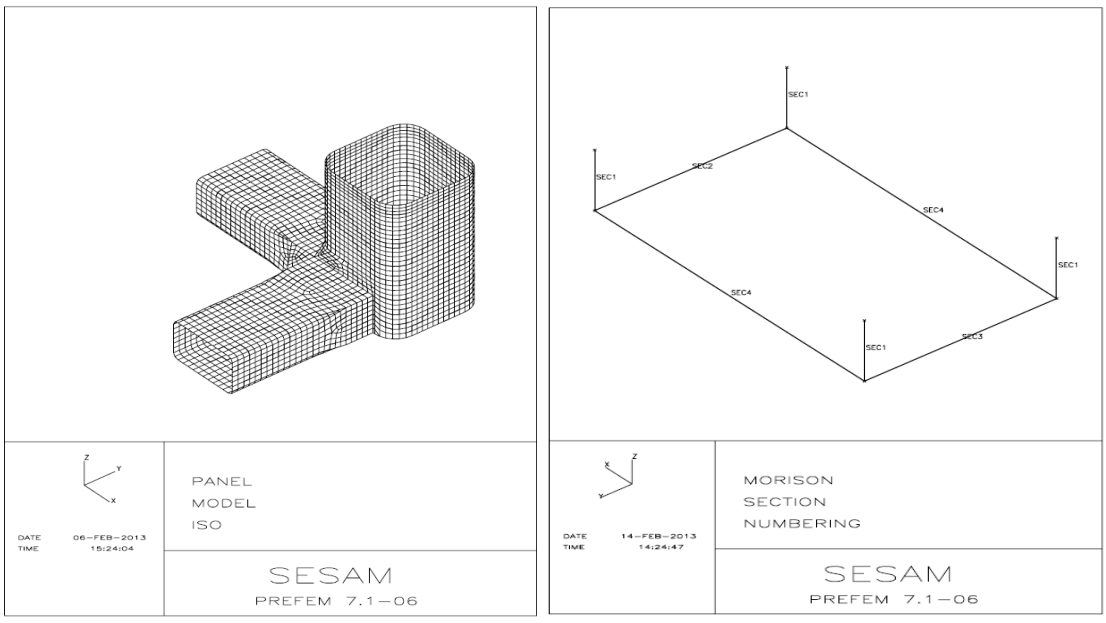

Figure 2.1 Example of panel model and slender element model

A catenary mooring system and a mass estimation are combined with the panel and the slender element model in the diffraction-radiation tool WADAM. The resulting transfer functions are combined with a sea state in POSTRESP. The sea state is

represented by the PIERSON-MOSKOWITZ spectrum in POSTRESP. The calculated motion characteristics include:

1. Eigenperiods and associated eigenvectors which are calculated in WADAM.

2. Static offsets calculated in the HYDA subroutine CATMOOR from the wind and current force coefficients combined with the mooring stiffness.

3. Stability at operation and in quay conditions.

4. Response amplitude operators for motions of six degree of freedoms due to waves propagating towards the bow, quartering sea and beam sea.

5. Calculated motion response and most probable minimum air-gap.

The key results of the calculation are combined with their respective target values to form an object function, which is the criterion for the program to assess the performance of the optimization. If the optimization option is activated, then HYDA uses the input parameter values as a starting guess and strives to minimize the object function via minimization algorithms. A SIMPLEX type of minimization algorithm is adopted here.

The analysis procedure mentioned above is summarized as a flow chart which is shown in Figure 2.2.

2.2 New contributions to the design tool

In this project, new contributions to the design tool HYDA are the modification of several sub-routines in the tool and studies of a non-conventional platform.

The modified subroutines include mass budget scaling, wind-force scaling, current-force scaling and mooring systems. The estimated mass budget is interpolated from two reference models. For wind-force resistance, data of one reference model from a wind tunnel test are considered in the same way as for mass budget. For mooring systems, mean drift forces are included in the subroutine for calculating static offset and line tension.

Motion responses of three different platforms are analysed using HYDA in this project, and special attention is paid to a special non-conventional unit. The design of the non-conventional unit is optimized in HYDA via the SIMPLEX algorithm in order to minimize the object function and the motion response.

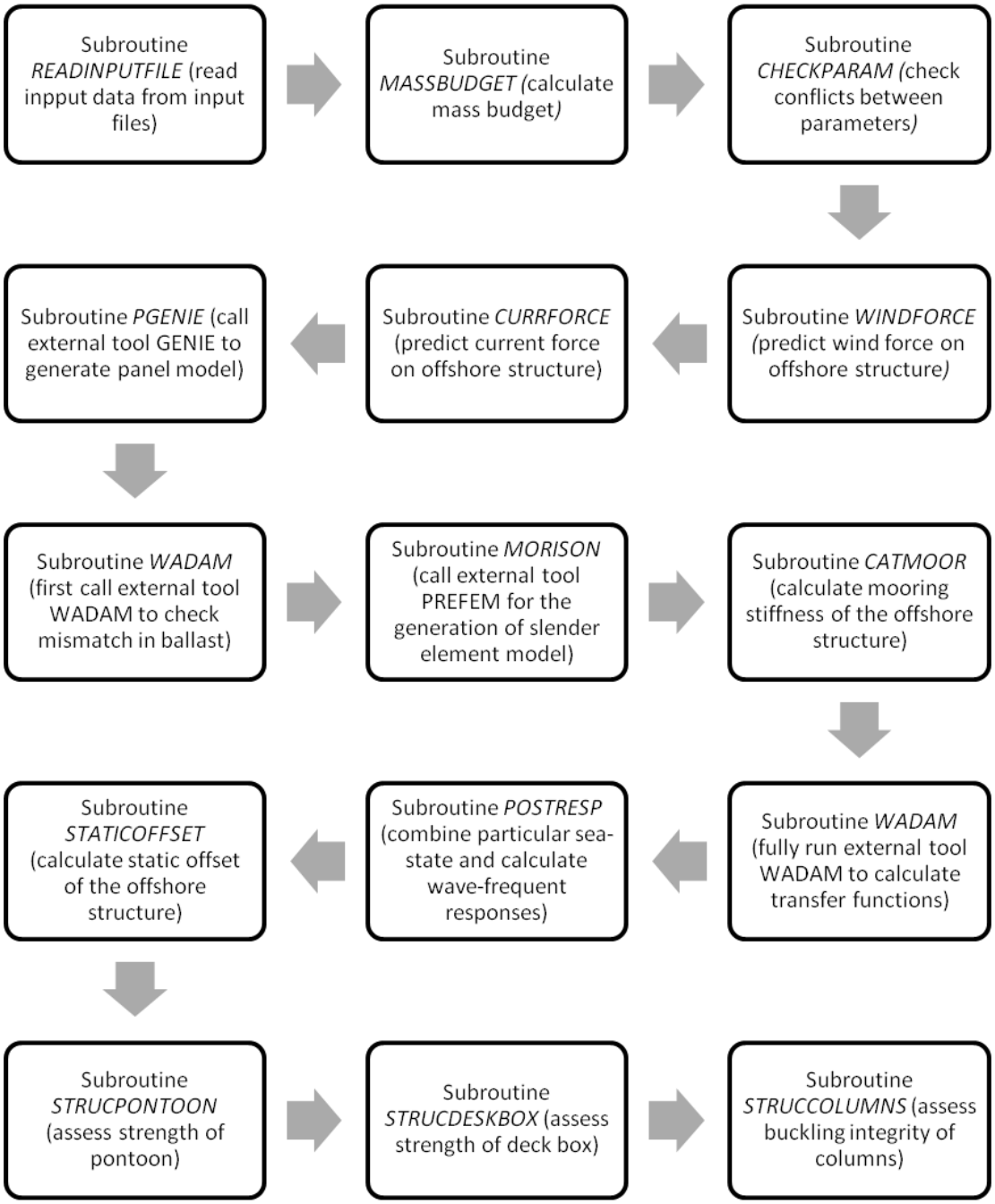

Figure 2.2 Flowchart of analysis procedure in HYDA

3 Environmental Conditions

Environmental conditions cover natural phenomena, which may contribute to structural damage, operation disturbances or navigation failures. The most important phenomena for marine structures are wind, waves and current.

3.1 Wind conditions

Wind speed varies with time and height above the sea surface. For theses reasons, the averaging time for wind speeds and the reference height must be specified. A commonly used reference height is $H = 10$ m. commonly used averaging time are 1 minute, 10 minutes and 1 hour. In this project, the average wind velocity over 1 hour at a height of 10 metres is adopted.

3.2 Current conditions

The current velocity vector varies with water depth. Close to the water surface the current velocity profile is stretched or compressed due to surface waves. However, in this project, the current is considered as a steady flow field and constant over depth.

3.3 Wave conditions

Short-term stationary irregular sea states may be described by a wave spectrum formulated by a set of parameters such as the significant wave height and peak period. In this project the *PIERSON-MOSKOWITZ* (PM) spectrum is adopted, which is given by:

$$S_{PM}(\omega) = \frac{5}{16} \cdot H_s^2 \omega_p^4 \omega^{-5} \exp\left(-\frac{5}{4} \left(\frac{\omega}{\omega_p} \right)^{-4} \right) \tag{3.1}$$

where ω is the wave frequency, H_s is the significant wave height, T_p is the peak period and $\omega_p = 2\pi / T_p$ is the angular spectral peak frequency,

4 Response Target

In order to distinguish a good design from a less good design we make use of typical design targets. Design targets are typically determined by customer requirements, equipment limitations and regulations.

In this chapter, the design target values of a non-conventional unit are introduced and they will be used in the optimization of a non-conventional unit in Chapter 12. The considered responses include:

- Heave amplitude, which is a critical criterion for the platform.
- Metacentric height, which represents the initial stability of the platform.
- Acceleration, which the human body is very sensitive to.
- Pontoon stress level, which indicates the strength of the pontoon.
- Mass of platform, which is related to the cost of the platform.
- Air gap, which is the distance between the wave crest and main deck of the platform.
- Static offset, which is the static displacement in the horizontal plane under wave, current and wind-force.
- Heel amplitude, which represents the static inclination under wind and current.
- Eigenperiod associated with heave motion, which indicates the probability that resonance happens.

The geometric dimension includes length, width or draught of platforms. Sometimes there are geometrical limitations in terms of dimension of a dry dock and water depth of the operation area. The length or width of floating platform is restricted due to width or length of dry dock. The draught of the platform could also be a restriction due to water depth of the sea, which often happens for a drilling unit since it is towed between different locations.

The target values of these responses are shown in Table 4.1. The calculated results are combined with their target values to form an objective function f defined as:

$$f = \sum_i a_i \left(\frac{X_i^{calculated} - b_i X_i^{target}}{X_i^{target}} \right)^2 \tag{4.1}$$

where:

$X_i^{calculated}$ is the calculated response.

X_i^{target} is the target response.

a_i and b_i are the weighting factors, which is defined by users according to the importance of the response in this optimization process. The default values are shown in Table 3.1. When the calculated result for a response fulfils the target values, a_i will automatically change to zero, and thus no values will be added to the objective function regarding this response.

The object function can partially reflect the difference between target values and calculation results. If the result of the object function is low then the design model may be close to target requirement. The case with the minimum value of the object function, which offers good results in all the considered responses, can be chosen as the optimized design.

Table 4.1 Design target values for a non-conventional unit and default value of weighting factors

Considered response and geometrical limits	Target value	a_i	b_i
Heave amplitude	≤2.0 m	2	0
Metacentric height	≥2 m	2	1
Acceleration	≤0.15g	1	1
Pontoon stress level	≤100 MPa	1	1
Displaced mass	≤10000 tonnes	2	1
Air gap	≥1.0 m	2	1
Heel amplitude	≤5.5°	2	0
Offset amplitude	≤7% of water depth	1	0
Eigen period associated with heave motion	≥22 s	---	---
Draught	30 m	2	0
Width	80 m	2	0

5 Reference Platform Models

In this Chapter, three different types of reference models are introduced and evaluated in HYDA. The geometric characteristic for each reference model is illustrated in Appendix 2, and here the typical computational results are shown and analysed.

5.1 Production unit

5.1.1 Geometric description and panel model

The geometry type of a production unit has the hull of a semi-submersible type providing a stable platform to support the topside. The hull itself consists of a ring pontoon with four columns, one in each corner, supporting a boxlike upper hull. The pontoons consist of a structure open to the sea. This is to avoid the hydrostatic pressure loads to the pontoons. Geometric input parameters of this unit are shown in Table 5.1.

In this section, a 4R (4 legs outside rectangular ring pontoon) type production unit has been analysed and the panel model is shown in Figure 5.1.

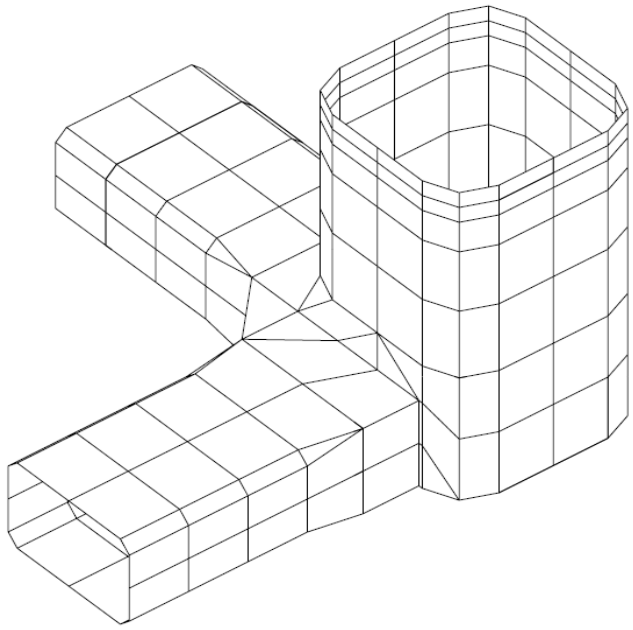

Figure 5.1 Panel model of the production unit

Table 5.1 Geometric input parameters

Length over columns	116 m
Length over pontoons	105 m
Width over columns	115 m
Draught	41.5 m
Keel to box bottom	61.5 m
Column radius	5 m
Column side	23 m
Pontoon height	11.5 m

5.1.2 Environmental conditions

In the analysis of the production unit, the following environment conditions have been adopted to represent a 100-year return period for the fictitious location:

- Water depth of location: 2130 m
- Significant wave height: 14.7 m
- Minimum peak period: 11.0 s
- Maximum peak period: 14.8 s
- Wind velocity: 39.0 m/s
- Surface current: 1.58 m/s

5.1.3 Computational result

The heave Response Amplitude Operator (RAO) of the production unit is shown in Figure 5.2 and the relevant computational results are listed in Table 5.2. Here, the metacentric height, acceleration and air-gap are relatively high in general.

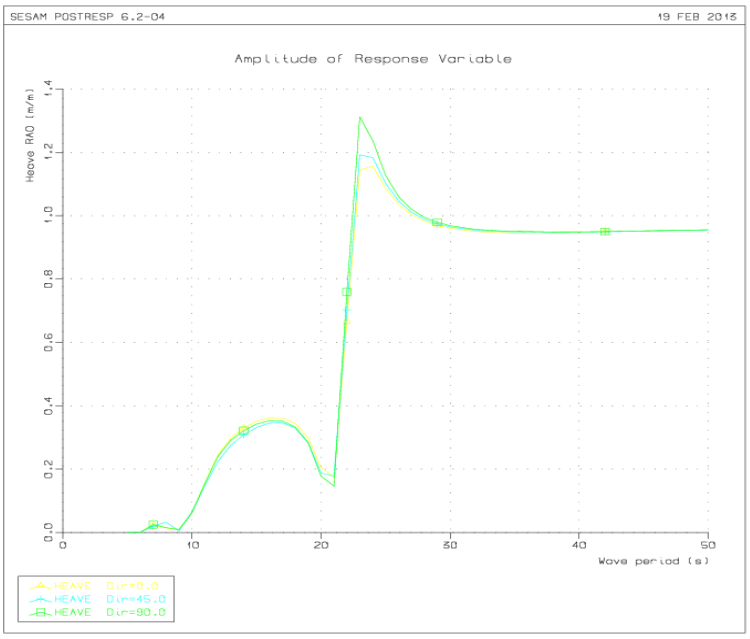

Figure 5.2 Heave RAO of Production unit

Table 5.2 Calculation results for the production unit

Considered response	Results from analysis model
Heave amplitude	3.5 m
Metacentric height	8.9 m
Acceleration	0.7g
Stress level	256 MPa
Displaced mass	143000 tonnes
Air gap	12.1m
Heel amplitude	6.4˚
Offset amplitude	6.9% of water depth
Eigen period associated with heave motion	22.7 s

5.2 Drilling unit

5.2.1 Geometrical description and panel model

An offshore drilling unit can move to different locations for a drilling operation. Here, a drilling unit (D4) is analysed using HYDA. A panel model of this unit is shown in Figure 5.3. Geometric input parameters of this unit are shown in Table 5.3.

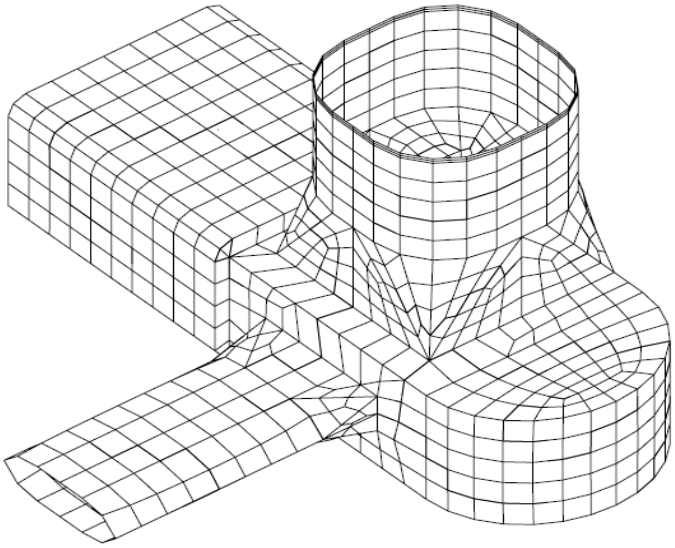

Figure 5.3 Panel model of the drilling unit

Table 5.3 Geometric input parameters

Length over pontoons	89.7 m
Pontoon height	9.1 m
Width over columns	70.7 m
Draught	25 m
Keel to box bottom	35.9 m
Column radius	5 m
Column side	13.7 m
Width of wing	10 m
Wing height	3 m

5.2.2 Environmental conditions

In the analysis of the drilling unit, the following environmental conditions have been adopted to represent a 100-year return period for the fictitious location:

- Water depth of location: 500 m
- Significant wave height: 13.4 m
- Minimum peak period: 11.5 s
- Maximum peak period: 15.0 s
- Wind velocity: 26.7 m/s
- Surface current: 0.6 m/s

5.2.3 Computational result

The heave Response Amplitude Operator (RAO) of the drilling unit is shown in Figure 5.4 and the selected computational results are listed in Table 5.4. Here, the heave amplitude and acceleration are rather high, which may affect the drilling operation. Also an unexpected negative air-gap occurred, which may result in a wave-in-deck force and structural damage may occur.

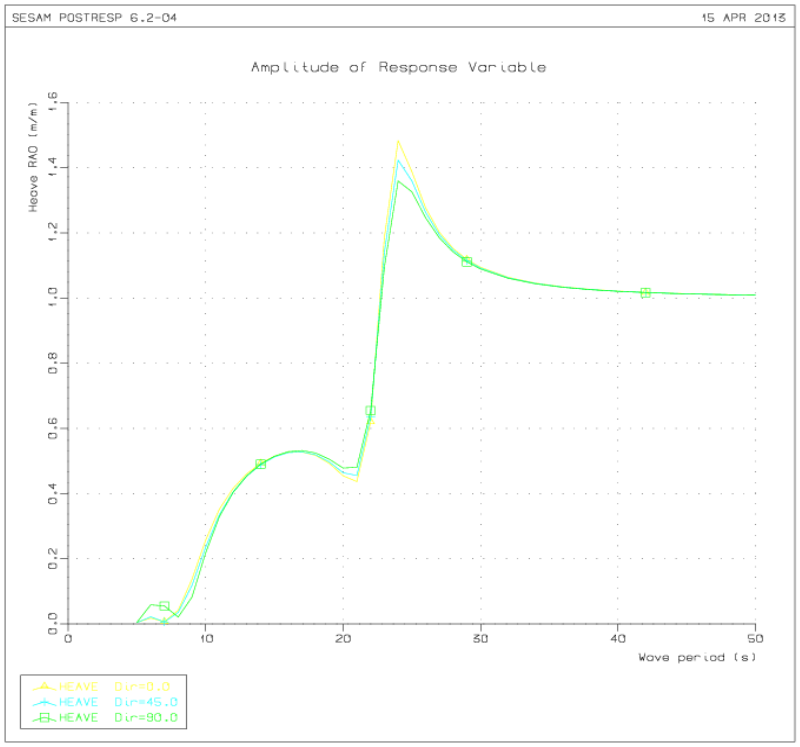

Figure 5.4 Heave RAO of drilling unit

Table 5.4 Calculation results for the drilling unit

Considered response	Results from analysis model
Heave amplitude	5.1m
Metacentric height	1.0 m
Acceleration	1.1g
Stress level	75 MPa
Displaced mass	39000 tonnes
Air gap	-2.1 m
Heel amplitude	5.4˚
Offset amplitude	6.4% of water depth
Eigen period associated with heave motion	23.6 s

5.3 The non-conventional unit

5.3.1 Geometric description and panel model

This section is devoted to the study of a non-conventional unit. The non-conventional semi-submersible structure includes a platform supported by columns and the pontoons disposed inboard between the columns as well as longitudinally outboard extension of the columns. A panel model of the considered non-conventional unit (U2) is shown in Figure 5.5. Geometric input parameters of this unit are shown in Table 5.5.

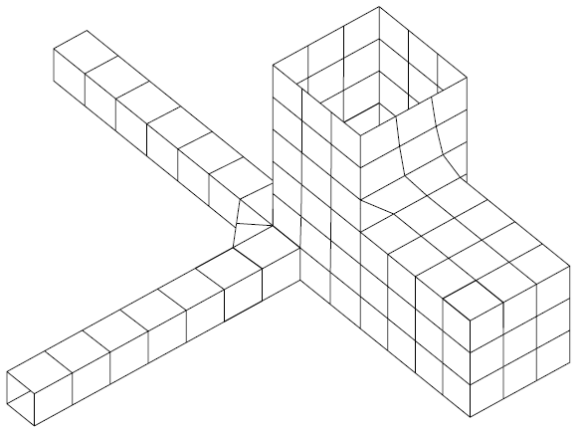

Figure 5.5 Panel model of the non-conventional unit

Table 5.5 Geometrical input parameters

Length over pontoons	90 m
Pontoon height	5 m
Pontoon width	5 m
Draught	30 m
Keel to box bottom	40 m
Front height	15 m
Front width	15 m
Column side	16 m
Width of wing	5 m

5.3.2 Environmental conditions

In the analysis of the non-conventional unit in Chapters 5 and 12, the following data is adopted to represent a 100-year return period for the fictitious location:

- Water depth of location: 500 m
- Significant wave height: 14.0 m
- Minimum peak period: 11.0 s
- Maximum peak period: 14.0 s
- Wind velocity: 26.67 m/s
- Surface current: 0.63 m/s

5.3.3 Computational result

The heave RAO of the non-conventional unit is illustrated in Figure 5.6 and the comparison between calculated results and the target values for non-conventional unit is listed in Table 5.6. From Figure 5.6 it can be seen that this type of platform has a good performance in terms of heave motion. But the main problems are the large negative air-gap and also the large width and low eigenperiod.

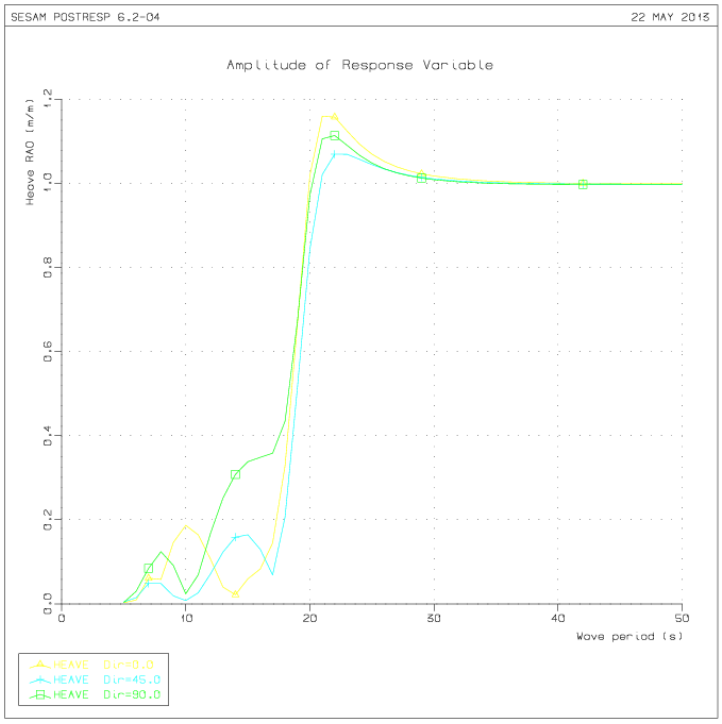

Figure 5.6 Heave RAO of a non-conventional unit

Table 5.6 Comparison between calculated results and target values for non-conventional unit

Considered responses and geometrical limits	Results from analysis model	Target value
Heave amplitude	3.27 m	≤2.0 m
Metacentric height	13.2 m	≥2 m
Acceleration	0.66g	≤0.15g
Stress level	1825 MPa	≤100 MPa
Displaced mass	59000 tonnes	≤10000 tonnes
Air gap	-7.2 m	≥1.0 m
Heel amplitude	3.9˚	≤5.5˚
Offset amplitude	6.7% of water depth	≤7% of water depth
Eigen period associated with heave motion	19.8 s	≥22 s
Width	112 m	80 m
Draught	30 m	30 m

6 The Influence of Panel Size

During the analysis, the panel size may have a significant effect on the final result. If the overall mesh size of the panel model is decreased to 5m from 10m in the tertiary input data, the program takes 4 or 5 minutes longer to analyse the model without optimization and the wind-force coefficients, current force coefficients, mass budget, metacentric height and mooring stiffness are not changed because these values are not sensitive to the mesh size of the panel. But the values of the eigenperiod and eigenvector, RAO, accelerations and air gaps are slightly changed because with the small mesh size the results can be more precise. However, if the mesh size is taken to a small value (i.e. 3m or 2m), it takes longer (more than 2 hours where the actual time is 5 or 10 minutes) to analyse the model without optimization, and the there are no significant changes in the results.

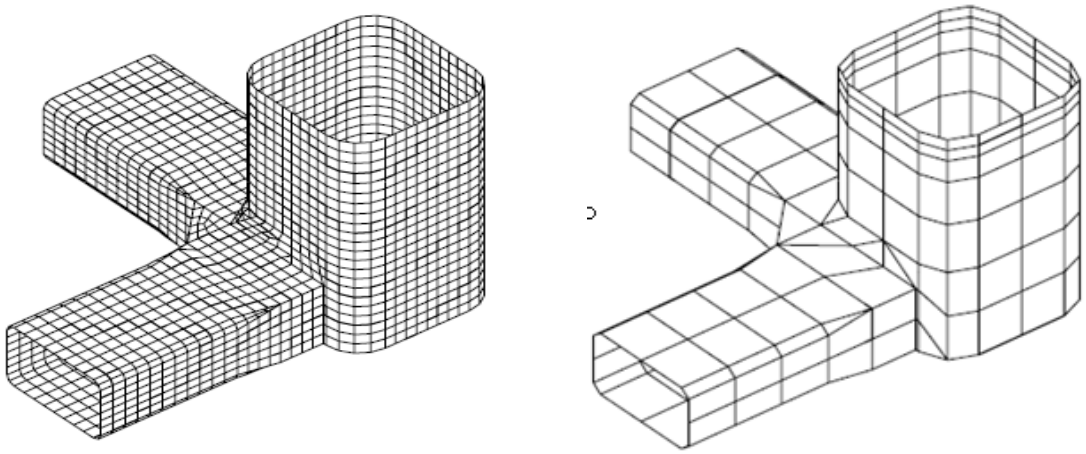

Figure 6.1 Production units panel model with a mesh size of 10 m and 2m, respectively

Some of the important results are shown below to visualize the differences in different panel size in Table 6.1.

Table 6.1 Comparison of different mesh sizes

Mesh size (m)	CPU time (minute)	Heave amplitude (m)	Mass (tonnes)	Acceleration (g)	Eigen period heave (s)
1.5	--	3.35	145000	0.63	23.8
2	120-130	3.46	144372	0.65	23.7
5	10-15	4.85	143203	0.83	24.2
10	5-10	3.53	143203	0.69	22.7

7 Mass Budget Scaling

The mass, the centre of the gravity and the radii of gyration with respect to the still water line are estimated in the subroutine MASSBUDGET, which is based on a typical minimum equipment list and geometric dimensions.

The mass of some items of the floating platform is regarded as primary input data in the program, and for remaining items the mass will be generated via the subroutine MASSBUDGET. It is necessary to use some scaling factors and reference values to generate the mass of the remaining items in the equipment list subroutine of the program. These scaling factors and the reference values are based on experience and existing platform design.

7.1 Existing mass budget scaling

In the initial mass budget, only one model is referred to as a reference model and it is assumed that there is a linear relationship between the reference model and the studied model. Items of the floating platform are listed in Appendix 3, which illustrates how their mass is scaled in the subroutine *equipmentlist1*. Here, the scaling of the equipment mass is illustrated as an example and the scaling formula is given as follows:

$$E = E_1 \times \frac{T}{T_1} \tag{7.1}$$

where E is the equipment mass of the studied model, E_1 is the equipment mass of the reference model. T is the topside mass of the studied model, T_1 is the topside mass of the reference model.

The existing mass budget for each item is tabulated in Appendix 3.

7.2 New contributions to mass budget scaling

It is not always appropriate to estimate the mass of different items only based on one reference model, since it is very probable that there is a significant difference between the reference model and the estimated model. So it is favourable to make a further investigation into improving the accuracy of mass scaling.

7.2.1 New created functions for mass budget

One possible solution for the mass budget is to establish the estimation function based on two reference models. The piecewise function is adopted and in order to set an upper limit to make the estimation more reasonable, the *arctan* function is adopted. The piecewise function is continuous from zero to infinity and the result of the prediction is dependent on the reference models.

The updated equipment mass is scaled as follows:

If $T \le T_1$:

$$E = \frac{(E_1 - 0)}{(T_1 - 0)} \times T \tag{7.2}$$

If $T \ge T_2$:

$$E = (E_{ul} - E_2) \times (2/\pi) \times \arctan\left(\frac{T}{sT_2} - \frac{1}{s}\right) + E_2 \tag{7.3}$$

If $T_1 < T < T_2$:

$$E = \frac{(E_2 - E_1)}{(T_2 - T_1)} \times (T - T_1) + E_1 \tag{7.4}$$

where E_{ul} is the upper limit of the equipment mass for the studied model, E_2 is the equipment mass of second reference model. T_2 is the topside mass of the second reference model, s is the factor for controlling the slope of the function.

Figure 7.1 shows the predicted equipment mass versus the different given topside mass. The updated mass budget for different items is listed in Appendix 4.

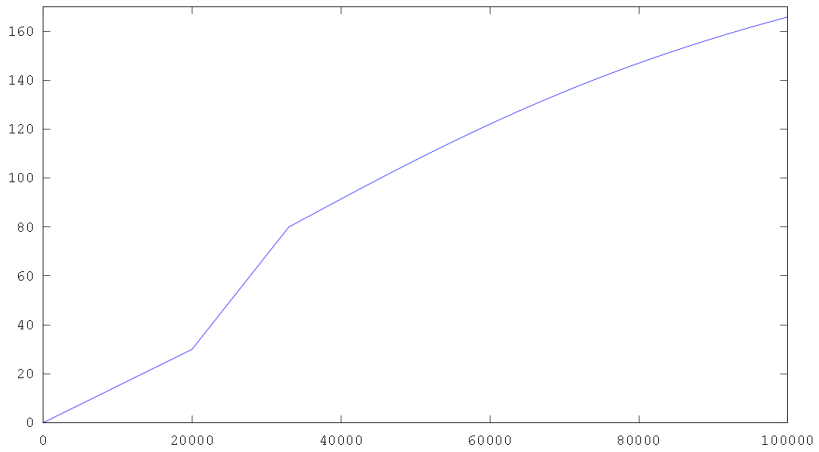

Figure 7.1 The predicted equipment mass vs. the given topside mass

7.2.2 Modification of the relevant source code

Based on the updated mass budget functions, the source code of subroutine *equipmentlist1* is updated. The reference models can be predefined or defined by the users. There will be a new integer variable *imass* in the program to control the option. If $imass = 1$, the two reference models will be defined by users. Or $imass = 0$, in which case the predefined reference models will be used. The reason for setting this variable is that if the user has better reference models, which are closed to the

designed one, they should be adapted since models with similar geometry and dimension will definitely give a better prediction of mass budget.

7.2.3 Limitations

The updated subroutine for mass budget scaling has some limitations and they will be discussed in this section.

1. In the input file of the reference models, the order of the row cannot be changed. This is mainly due to the fact that the program reads the input data and assigns the value to the variables in a fixed way. If the order of the input data is changed, the variables will be assigned the wrong values.

2. The name of the input data should not be changed. The names of the input data for reference models are *ref_model1.inp* and *ref_model2.inp*. They cannot be substituted with any other names, since the source code only opens the files with these two names. If they do not exist, the program will be stopped.

3. The data of these two reference models should be reliable enough and similar to the designed model. The accuracy of the prediction is to a large extent dependent on the reference models.

8 Wind Force Scaling

8.1 Wind loads on offshore structures

Wind-induced loads are in general time-dependent loads due to fluctuations in wind velocity. The response of a structure due to wind loading can be partitioned into a static and a dynamic contribution. Only the static response is accounted for here.

The wind pressure can be described by the following relationship (cf. DNV (2010)):

$$q = \frac{1}{2}\rho_a U_{T,z}^2 \tag{8.1}$$

where q is the wind pressure, ρ_a is mass density of air which is to be taken as 1.2 kg/m^3. Moreover, $U_{T,z}^2$ is the wind velocity averaged over a time T at a height z metres above the mean water level.

The wind force F_w on a structure member is formulated as:

$$F_w = CqS \tag{8.2}$$

where C is the shape coefficient and q is the wind pressure as defined in equation (8.2) and S is the projected area of the member normal to the direction of the force.

In this project, the projected area exposed to wind is not a previously known variable. The adopted wind force coefficients $k_w = 1/2\rho_a CS$ are based on similar projects scaled with respect to geometric dimensions (e.g. projected area S) in the subroutine WINDFORCE.

8.2 Existing wind-force scaling

Similar to mass budget scaling, wind-force coefficients for different motions in different directions are also scaled, based on some scaling factors and reference values. These scaling factors and reference values are also taken based on existing floating platforms. In the initial wind-force resistance scaling, surge force is scaled with the multiplication of width and static air-gap, which can be roughly approximated as an exposed area of the platform and only one reference model is referred to. Sway force, pitch moment and roll moment are calculated based on the surge force.

Here, the wind-force coefficient in a head direction for the surge response of the studied model is illustrated as an example:

$$F_w = 4.58 \times W_p \times SAG / (W_{p1} \times SAG_1) \tag{8.3}$$

Where SAG is the static air-gap of the studied model, W_p is the width over column of the studied model, W_{p1} is the width over column of the reference model and SAG_1 is the static air-gap of the reference model.

The wind-force coefficients for different motions in each direction are tabulated in Appendix 5.

8.3 New contributions to wind-force scaling

8.3.1 New created function for wind-force scaling

Factors which have influence on wind-force resistance are the wind area of a derrick, topside module, deck box and column side along with their shape. These factors should be accounted for in an updated subroutine.

Surge and sway force are proportional to the front and side area of the platform, respectively. Piecewise functions are established based for interpolation between two reference models. The pitch and roll moment can be regarded as a surge and sway force times their levers. The lever can be approximated as the multiplication of static air-gap and a scaling factor. This scaling factor is motivated from trends in experimental wind tunnel data. The detailed formula can be referred to in Appendix 6.

The updated wind-force coefficient in a head direction for surge response is estimated via the following formulas:

If $A_f \le A_{f_1}$:

$$F_w = \frac{(F_{w1} - 0)}{(A_{f1} - 0)} \times A_f \tag{8.4}$$

If $A_f \ge A_{f_1}$:

$$F_w = (F_{wul} - F_{w2}) \times (2/\pi) \times \arctan\left(\frac{A_f}{sA_{f2}} - \frac{1}{s}\right) + F_{w2} \tag{8.5}$$

If $A_{f_1} < A_f < A_{f_2}$:

$$F_w = \frac{(F_{w2} - F_{w1})}{(A_{f2} - A_{f1})} \times (A_f - A_{f1}) + F_{w1} \tag{8.6}$$

where $A_f, A_{f1}\ A_{f2}$ are the front areas of the studied model - the first and second reference model above water. $F_w, F_{w1}\ F_{w2}$ are the wind-force coefficients of the studied model - the first and second reference model. s is the factor for controlling the slope of the function. F_{wul} is the upper limit for the wind-force coefficient.

8.3.2 Modification of the relevant source code

Similar manners are adopted in the subroutine for wind resistance scaling. The user will determine if user-defined reference models or predefined reference models will be adopted by defining the value of variable *imass*. The new created functions have been introduced in the program. At the same time in the input file, three new items have been added, namely the the exposed area of the derrick, the topside module and the deck box height. They will be recognized by the program through the subroutine *readinputfile.*

8.3.3 Limitations

1. The true lever for pitch and roll moments are approximated as a multiplication of the scaling factor and static air-gap of the floating platform. Thus, it is not always accurate for different kinds of platforms.

2. The factor is predefined in the program and therefore fixed for all types of platforms. But the value of the factor is derived from regular semi-submersibles so there will be errors for other types of platforms.

3. For user-defined reference models, detailed data from the reference model are required, such as the derrick area, the topside module area, etc. Also, data for these two reference models should be reliable since it will determine the accuracy of the wind resistance scaling being to a large extent dependent on the reference models.

9 Current Force Calculation

9.1 Current loads on offshore structures

The effects of currents should be considered for the design, construction and operation of offshore structures. Current loads on a semi-submersible structure can be regarded as the sum of the current load on pontoons and columns.

Normally, pontoons and columns can be regarded as slender members that satisfy the following condition:

$$\lambda > 5D \tag{9.1}$$

where λ is the wave length, typically in the following Chapter 12 for an analysis of a non-conventional unit, it is 342 metres and D is the diameter or other projected cross section dimension of the member.

For fixed slender structural members in current having cross sectional dimensions sufficiently small to allow the gradients of fluid particle velocities and accelerations in the direction normal to the member to be neglected, current loads may be calculated using Morison's load formula being a sum of an inertia force proportional to accelerations and a drag force being proportional to the square of velocity:

$$f_N(t) = \rho(1+C_A)A\dot{v} + \frac{1}{2}\rho C_D D v|v| \tag{9.2}$$

The following definitions apply for Equation (9.2):

$$C_D = \frac{f_{drag}}{\frac{1}{2}\rho D v^2} \tag{9.3}$$

$$C_A = \frac{m_a}{\rho A} \tag{9.4}$$

Where

v = fluid particle velocity [m/s]

$\dot{v}$ = fluid particle acceleration [m/s^2]

A = cross section area [m^2]

D = diameter or typical cross section dimension [m]

ρ = mass density of fluids [kg/m^3]

f_{drag} = sectional drag force per unit [N/m]

m_a = the added mass per unit length [kg/m]

C_A = added mass coefficient

C_D = drag coefficient

In general, the fluid velocity vector will be in a direction relative to the axis of the slender member, see Figure 9.1. The drag force f_{drag} is decomposed in a normal force f_N and a tangential force f_T. The added mass is already calculated in a panel model, so here only viscous force is accounted for. The current force coefficient used in subroutine CURRFORCE can be defined as:

$$k_c = \frac{1}{2}\rho C_D D \tag{9.5}$$

where C_D and D are defined above in Equation (9.2) and (9.3).

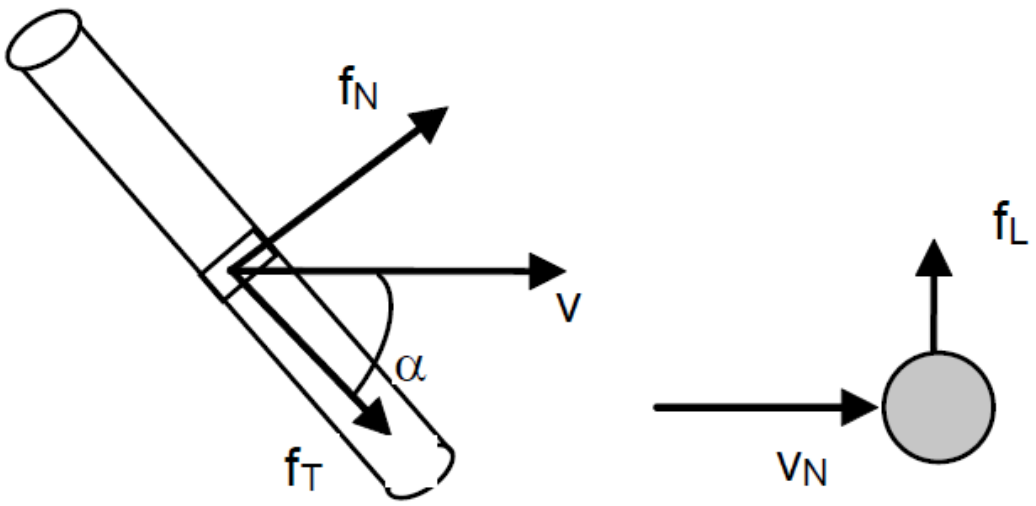

Figure 9.1 Definition of normal force, tangential force and lift force on a slender structure (DNV (2010)).

9.2 Existing current force calculation

In the current force resistance calculation - an unlikely mass budget and wind force scaling - it is not scaled compared to any reference model. It is calculated directly via a Morison Equation and C_D values are listed in Appendix 7 and formulas for existing current force calculation are given in Appendix 8.

Here, the head current force coefficient for a surge response of the studied model is given as an example for explaining the adopted method:

$$F_c = (4 \times scol \times D + 2 \times spon \times W_p) / 2 \tag{9.6}$$

The following definitions apply in Equation (9.6):

$$scol = C_{dcol} \frac{\rho}{2} L_c \tag{9.7}$$

$$spon = C_{dpon} \frac{\rho}{2} H_p \tag{9.8}$$

where D is the draught of the column, W_p is the width over columns, C_{dcol} is the drag coefficient for columns, C_{dpon} is the drag coefficient for pontoons, L_c is the column side length and H_p is the pontoon height.

9.3 New contributions to current force calculation

9.3.1 Modification on current force calculation

A Morison equation gives a good result in the estimation of the viscous effect on pontoons and columns. In the modified subroutine, surge force and pitch moment are kept unchanged and a small modification has been made for the sway and roll response.

For example, the current force coefficient in the quarter direction for a sway response of the studied model is as follows:

$$F_c = (4 \times scol \times D + 2 \times spon \times L_p) \times R_p / 2.4 \tag{9.9}$$

where L_p is the length over column, R_p is the pontoon height ratio. For a drilling unit with 4 legs and a non-conventional unit with 4 legs and box appendices, R_p is defined as the ratio of the pontoon height and wing height. For other types of semi-submersibles, it is equal to 1.

The detailed formula for the current force modification can be referred to in Appendix 9.

9.3.2 Limitations

For the calculation of current force coefficients, there are a couple of limitations that should be observed:

1. Wake interaction is not accounted for in the calculation of current force. For a regular semi-submersible platform, there should be four columns, two of which are in the upstream of the incident flow and another two are in the downstream. The force on the cylinder downstream of another cylinder upstream is influenced by the wake generated by the upstream cylinder. The

main effects on the mean forces on the downstream cylinder is the reduced mean drag force due to shielding effects and the non-zero lift force due to velocity gradients in the wake field. But in subroutine CURRFORCE, this effect is not included. However, regarding drag force, it is a conservative estimate if taken out of the vortex shielding.

2. The Current load is considered to be separated from the wave load. WADAM has a limitation that can only be solved by a linear equation , so coupled effects of waves and currents are not accounted for in WADAM.

10 Mooring Systems

10.1 Introduction to mooring systems

The precise positioning and long-term motion control of offshore structures are important in offshore operations. Mooring systems are one major tool for maintaining offshore structures in position in a current and in the wind and waves.

Typical important mooring systems include:

1. A catenary-line mooring, which derives its restoring force primarily by lifting and lowering the weight of the mooring line. Generally, this yields a hard spring system with a force increasing more than directly proportional to the displacement. In a spread mooring system, several pre-tension anchor lines are arrayed around the structure to hold it in the desired location. The anchors can not be loaded by too large vertical forces so that it is necessary that a significant part of the anchor line lies on the seabed.

2. A taut-line mooring, which has a pattern of taut, lightweight lines radiating outward. The lines have a low net submerged weight and the catenary action has been eliminated.

3. A tension-leg mooring, which is specially used for tension-leg platforms.

In this project only catenary-line mooring systems are analysed and discussed since they are the most commonly used mooring systems in offshore structures.

10.2 Static analysis of mooring systems

10.2.1 Static analysis of a cable line

For static analysis of a cable line, it is assumed that a horizontal seabed and the cable is in a vertical plane coinciding with the x-z plane. Bending stiffness and dynamic effects in the line are not considered.

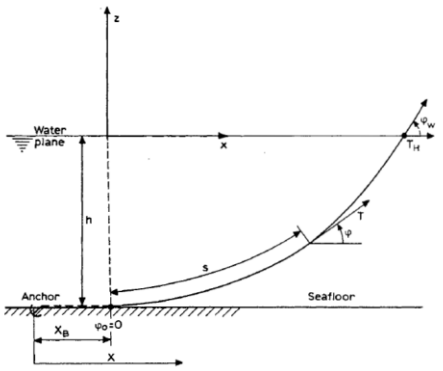

Figure 10.1 Coordinate systems in the analysis of cable line (cf. Faltinsen (1993))

Figure 10.1 shows the coordinate systems, which, defined in this problem and in Figure 10.2, show one element of the cable line. Forces D and F acting on the element are the mean hydrodynamic forces per unit length in the normal and tangential direction, respectively. Here, w is the weight per unit length of the line in water, A is the cross section area of the cable line, E is the elastic modulus and T is the line tension.

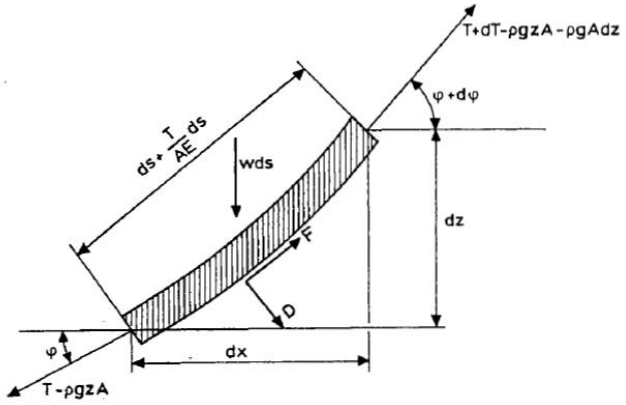

Figure 10.2 Forces acting on one element of the cable line (cf. Faltinsen (1993))

The equilibrium relationship along the segment and perpendicular to the segment can be established as in the following equations (cf. Faltinsen(1993)):

$$dT - \rho gAdz = \left[w\sin\phi - F\left(1 + T/(AE)\right)\right]ds \tag{10.1}$$

$$Td\phi - \rho gAzd\phi = \left[w\cos\phi + D\left(1 + T/(AE)\right)\right]ds \tag{10.2}$$

These equations are non-linear equations and it is generally not possible to find an explicit solution. However, for many operations it is a good approximation not to consider the current force D and F. Moreover, the effect of elasticity can also be neglected in order to simplify the analysis. By introducing these assumptions, the following equations can be derived:

$$dT' = w\sin\phi ds \tag{10.3}$$

$$T'd\phi = w\cos\phi ds \tag{10.4}$$

where

$$T' = T - \rho gA \tag{10.5}$$

Dividing Equation (10.3) by Equation (10.4), it can be seen that:

$$\frac{dT'}{T'} = \frac{\sin\phi}{\cos\phi}d\phi \tag{10.6}$$

Integrating the equation in both sides:

$$\int_{T_0'}^{T'} \frac{dT'}{T'} = \int_{\phi_0}^{\phi} \frac{\sin\phi}{\cos\phi} d\phi \tag{10.7}$$

the following equation can be obtained:

$$T' = T_0' \frac{\cos\phi_0}{\cos\phi} \tag{10.8}$$

Substituting Equation (10.8) for T' in Equation (10.4) and integrating Equation (10.4):

$$s - s_0 = \frac{1}{w} \int_{\phi_0}^{\phi} \frac{T_0'}{\cos\theta} \frac{\cos\phi_0}{\cos\theta} d\theta = \frac{T_0' \cos\phi_0}{w} \left(\tan\phi - \tan\phi_0\right) \tag{10.9}$$

Since $dx = \cos\phi ds$, Equation (10.9) can be written as:

$$\int_{\phi_0}^{\phi} \frac{dx}{\cos\theta} = \frac{1}{w} \int_{\phi_0}^{\phi} \frac{T_0'}{\cos\theta} \frac{\cos\phi_0}{\cos\theta} d\theta \tag{10.10}$$

which results in the following relationship:

$$x - x_0 = \frac{T_0' \cos\phi_0}{w} \left[\log\left(\frac{1}{\cos\phi} + \tan\phi \right) - \log\left(\frac{1}{\cos\phi_0} + \tan\phi_0 \right) \right] \tag{10.11}$$

Also in the same way since $dz = \sin\phi ds$:

$$z - z_0 = \frac{T_0' \cos\phi_0}{w} \left[\frac{1}{\cos\phi} - \frac{1}{\cos\phi_0} \right] \tag{10.12}$$

Here, ϕ_0 is the point of contact between the cable line and the seabed, as stated in Section 10.1, $\phi_0 = 0$. From Equation (10.8):

$$T_0' = T' \cos\phi \tag{10.13}$$

The horizontal component of the tension at the water plane can be written as:

$$T_H = T \cos\phi_w \tag{10.14}$$

By comparing Equations (10.5), (10.13) and (10.14) it can be seen that:

$$T_0' = T_H \tag{10.15}$$

Then, according to the boundary conditions, which indicate that $x_0 = 0$, $z_0 = -h$ and $s_0 = 0$, Equation (10.11) can be rewritten:

$$\frac{xw}{T_H} = \log\left(\frac{1+\sin\phi}{\cos\phi}\right) \tag{10.16}$$

i.e.

$$\sinh\left(\frac{xw}{T_H}\right) = \frac{1}{2}\left(\frac{1+\sin\phi}{\cos\phi} - \frac{\cos\phi}{1+\sin\phi}\right) = \tan\phi \tag{10.17}$$

$$\cosh\left(\frac{xw}{T_H}\right) = \frac{1}{2}\left(\frac{1+\sin\phi}{\cos\phi} + \frac{\cos\phi}{1+\sin\phi}\right) = \frac{1}{\cos\phi} \tag{10.18}$$

Substituting it into Equations (10.9) and (10.12):

$$s = \frac{T_H}{w}\sinh\left(\frac{w}{T_H}x\right) \tag{10.19}$$

$$z + h = \frac{T_H}{w}\left[\cosh\left(\frac{w}{T_H}x\right) - 1\right] \tag{10.20}$$

Combining Equations (10.5), (10.13), (10.12) and (10.15), the line tension can be found:

$$T = T_H + wh + (w + \rho g A)z \tag{10.21}$$

Based on Equations (10.19) and (10.20), the length of the mooring line l_s can be written as:

$$l_s^2 = h^2 + 2ha \tag{10.22}$$

where

$$a = \frac{T_H}{w} \tag{10.23}$$

The mean position of the offshore structure in wind, waves and current can be formulated as follows (see Figure 10.3):

$$X = l - l_s + x \tag{10.24}$$

By using Equations (10.22) and (10.20), the relationship between X and T_H can be established:

$$X = l - h\left(1 + 2\frac{a}{h}\right)^{\frac{1}{2}} + a\cosh^{-1}\left(1 + \frac{h}{a}\right) \tag{10.25}$$

In actual fact, due to the motions of the structures in waves, the distance X will oscillate. If the horizontal motions are not too large, the horizontal force can be expressed as:

$$T_H = (T_H)_M + C_{11}\eta_1 \tag{10.26}$$

Here $(T_H)_M$ is the average horizontal force from the anchor line which is used in the previous derivation. η_1 is the horizontal motion of the x-direction at the point of the offshore structure where the cable is connected to it. By differentiating Equation (10.25) it follows that:

$$C_{11} = \frac{dT_H}{dX} = w\left[\frac{-2}{\left(1+2\frac{a}{h}\right)^{\frac{1}{2}}} + \cosh^{-1}\left(1+\frac{h}{a}\right)\right]^{-1} \tag{10.27}$$

So here $a = {(T_H)_M}/{w}$.

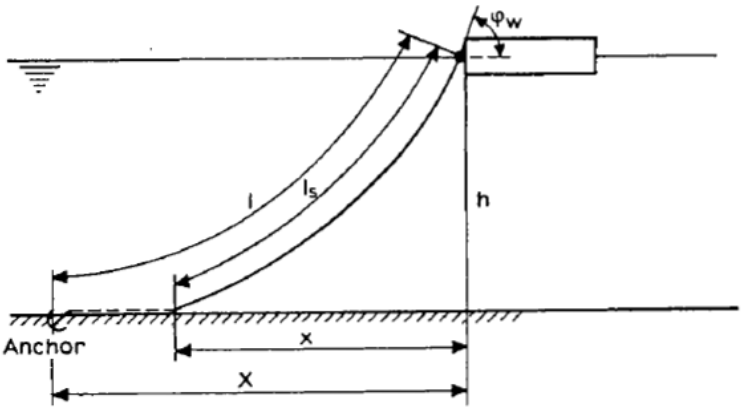

Figure10.3 Offshore structures moored with one anchor line (Faltinsen (1993))

10.2.2 Analysis of a spread mooring system

The above procedure for one cable line can be generalized in order to a spread mooring system consisting of several cable lines. Considering the contributions from each cable line separately, the horizontal forces and yaw moments can be formulated as:

$$F_1^M = \sum_{i=1}^{n} T_{Hi}\cos\psi_i \tag{10.28}$$

$$F_2^M = \sum_{i=1}^{n} T_{Hi} \sin\psi_i \tag{10.29}$$

$$F_6^M = \sum_{i=1}^{n} T_{Hi} \left[x_i \sin\psi_i - y_i \cos\psi_i \right] \tag{10.30}$$

where T_{Hi} is the horizontal force from anchor line number i. Its direction is from the attachment point of the anchor line towards the anchor. Furthermore, x_i and y_i are the x and y coordinates, respectively, of the attachment point of the anchor line to the offshore structure and ψ_i is the angle between the anchor line and the x-axis.

The restoring coefficients of the mooring systems can be formulated as:

$$C_{11} = \sum_{i=1}^{n} k_i \cos^2\psi_i \tag{10.31}$$

$$C_{22} = \sum_{i=1}^{n} k_i \sin^2\psi_i \tag{10.32}$$

$$C_{66} = \sum_{i=1}^{n} k_i \left[x_i \sin\psi_i - y_i \cos\psi_i \right]^2 \tag{10.33}$$

10.3 Existing subroutine for a mooring system

10.3.1 Mooring stiffness calculation

The mooring line stiffness is calculated via subroutine CATMOOR. It is calculated based on Equation (10.27) and the stiffness of the spread mooring system is calculated via Equations (10.31)-(10.33). An initial guess of pre-tension is made at the beginning of the subroutine and the horizontal component of the mooring line force is approximated equal to pre-tension. A loop is established in order to optimize the result and select a suitable mooring line. The diameter, mass and breakload of thirteen different kinds of mooring lines are provided in the program in the subroutine SCANROPE.

The pre-tension will increase step by step during iterations for each line until it is lager than breakload/1.5. Subsequently, this mooring line will be substituted by another one and repeat the above calculation. The criteria for stopping the loop is that the static offset is smaller than 7% of the water depth and the safety factor of each mooring line is lager than 2.7.

If the above criteria cannot be satisfied by all kinds of mooring lines, the program will automatically choose the stiffest mooring line.

10.3.2 Static offset calculation

The static offset and safety factor is calculated via the subroutine OFFSETCALC. The environment load in the program includes wind force and current force which can be introduced from subroutine WINDFORCE and subroutine CURRFORCE. The stiffness of the spread mooring systems is regarded as a constant and the static offset can be obtained as the load divided by the stiffness. It is only valid for a small offset.

The maximum line tension is calculated in the program based on Equation (10.21) where $z = 0$. The safety factor of each line is defined as the breakload divided by the line tension.

10.4 A modification of the subroutine for the mooring system

10.4.1 A modification of the subroutine for mooring stiffness

Originally, in the subroutine CATMOOR for the calculation of mooring systems, only four angles are proposed to be the possible angle combination of mooring line systems, which are 45˚, 135˚, 225˚ and 315˚. If the system consists of more than four lines, the multiplicator is introduced, which is defined as the number of mooring lines divided by 4. This multiplicator actually assumes that there will be more than one line in the same position and sharing same angle, which is unrealistic. Especially for a yaw motion, this assumption will lead to computation errors since yaw is sensitive to the angle combination.

Normally considering the number of mooring lines for a semi-submersible as being around 16, in the modified subroutine, 16 angles are proposed as the angle combination for a mooring line system while the multiplicator is changed to the number of mooring line divided by 16. The proposed angles are: 39˚, 43˚, 47˚, 51˚, 129˚, 133˚, 137˚, 141˚, 219˚, 223˚, 227˚, 231˚, 309˚, 313˚, 317˚ and 321˚.

10.4.2 A modification of the subroutine for a static offset

In the existing subroutine when calculating the wind and current forces which induce the platform offset, only the wind and current coefficients for surge are introduced. The coefficients for sway in head sea are simplified in the same as surge in beam, while coefficients for sway in beam are same as surge in head sea. For quarter sea, it is assumed that they have the same coefficients.

The assumptions above can result in a minor inaccuracy, so in the modified subroutine the wind and current coefficients for both surge and sway are introduced from subroutine WINDFORCE and subroutine CURRFORCE thus making the current and wind force independent of each other and improving accuracy.

11 The Mean Drift Force in Offset Calculation

11.1 The mean drift force on offshore structures

Environmental loads acting on offshore structures include wind, current and wave forces. So when calculating the static offset of offshore structures, the mean drift force should be included as part of the environmental force.

Drift force is induced by non-linear wave potential effects. The solution of the second-order problem results in a mean drift force and a force oscillating in a low-frequency region.

A simple example is shown here in order to explain the mean drift force. Assuming that a regular wave hits a vertical wall and is fully reflected, the time-average force acting on the wall can be calculated based on the following equation:

$$\overline{F} = \frac{1}{2}\rho g \varsigma_a^2 \tag{11.1}$$

where $\overline{F}$ is the mean drift force (time average force acting on the wall), ς_a is the amplitude of the incident wave. It can be seen from Equation (11.1) that when it is fully reflected, the drift force has a magnitude proportional to the square of the incoming wave amplitude and it is directed towards the wall, which is not the same as a linear solution. But, generally, only a part of the regular wave will be reflected and the rest will be transmitted underneath the floating body.

Normally, two methods can be adopted to derive the drift force: one is the conservation of momentum and another is the direct integration method. The detailed derivation using the direct integration method is given in Appendix 10 and here the mean drift force of an irregular wave has been directly adopted:

$$\overline{F}_i^s = 2\int_0^\infty S(\omega) Q_i^{WD}(\omega, \beta) d\omega \tag{11.2}$$

where $S(\omega)$ is the P-M sea spectrum as described in Section 3.3, $Q_i^{WD}(\omega, \beta)$ is the wave drift coefficient function for direction β and frequency ω. It can be defined as:

$$Q_i^{WD} = \frac{\overline{F}_i(\omega; \beta)}{\varsigma_a^2} \tag{11.3}$$

where $\overline{F}_i(\omega; \beta)$ are the mean wave loads in regular waves and ς_a is wave amplitude.

11.2 Calculation of the mean drift force in HYDA

In order to include the mean drift force when calculating the static offset of the offshore structure, a new subroutine MEANDRIFT is established. The transfer functions in 36 different frequency and 3 different headings are calculated via WADAM, based on both a momentum conservation method and a direct integration method. The results are listed in the output file *wadam.fca*.

In subroutine MEANDRIFT, the values of transfer functions based on the momentum conservation method are read into the program. The expression for numerical integration is formulated as:

$$\overline{F}_i^s(\beta) = 2\sum_{i=1}^{36}\left(\frac{S(\omega_i)+S(\omega_{i+1})}{2}\right)\left(\frac{Q_i^{WD}(\omega_i,\beta)+Q_i^{WD}(\omega_{i+1},\beta)}{2}\right)\cdot(\omega_i-\omega_{i-1}) \quad (11.4)$$

The integration is implemented in this subroutine and the mean drift force can be obtained. Statically, the total force can be represented as the sum of the current force, mean drift force and wind force. A new calculated static offset including the effect from the mean drift force is saved in the file *staticoffset.fca*.

12 Optimization of the Non-Conventional Unit

Based on the results in Section 5.3, it can be seen that the value of an objective function is still relatively high and the amplitude of many responses do not fulfil the requirements. In this chapter, in order to optimize the motion response and reduce the value of the objective function, the optimization of the non-conventional unit will be carried out in order to adjust the geometrical dimension of the platform.

12.1 Optimization algorithm

The criteria for selecting a pertinent optimization algorithm are robustness and performance. Robustness is used in the meaning that the algorithm shall work on all geometry types in the model library and not stop optimization unless it is stopped manually. Performance means a high rate of convergence throughout the optimization. Basically, it rules out gradient-based algorithms that primarily work in the vicinity of a local minimum. According to the criteria listed above, the Simplex method is selected and combined with a grid-based selection of start guesses.

12.2 Framework of the analysis

A deep-water floating system is an integration-dynamic system of a floater, risers and moorings responding to wind, wave and current loading in a complex way. Thus, different analysis methods are proposed to account for the interaction and coupled effects between slender structures and large volume floaters become significant. In this chapter, for the analysis of the non-conventional unit, the following analysis method is selected.

12.2.1 Analysis domain

A frequency domain analysis is carried out in this chapter. The transfer functions are generated in WADAM and it is the basis for frequency-dependent excitation forces (1^{st} and 2^{nd} order), added mass and damping.

12.2.2 Motion time scale

A floating moored structure may respond to environment loads on three different time scales: wave frequency motions, low-frequency motions and high-frequency motions. Here, in this analysis only a wave frequency motion is considered.

12.2.3 Coupling effects

Coupling effects refer to the influence on the floater mean position and dynamic response from a slender structure restoring, damping and inertia force.

The analysis is considered to be de-coupled. The equations of the rigid body floater motions are solved in the frequency domain. The effects of the mooring are included

quasi-statically using non-linear springs. Riser effects are disregarded here. For other coupling effects, for example contributions from damping and current loading on the mooring line, are not considered here.

12.3 Optimization of a non-conventional unit

The U2 type non-conventional unit, which is the same with the model in Section 5.3, is analysed with optimization. The key responses versus iterations are shown in Figure 12.1 and it is obvious that all the important responses converge at the end of the optimization when it reaches 450 iterations. The specific iteration with the lowest objective value is selected and analysed in detail.

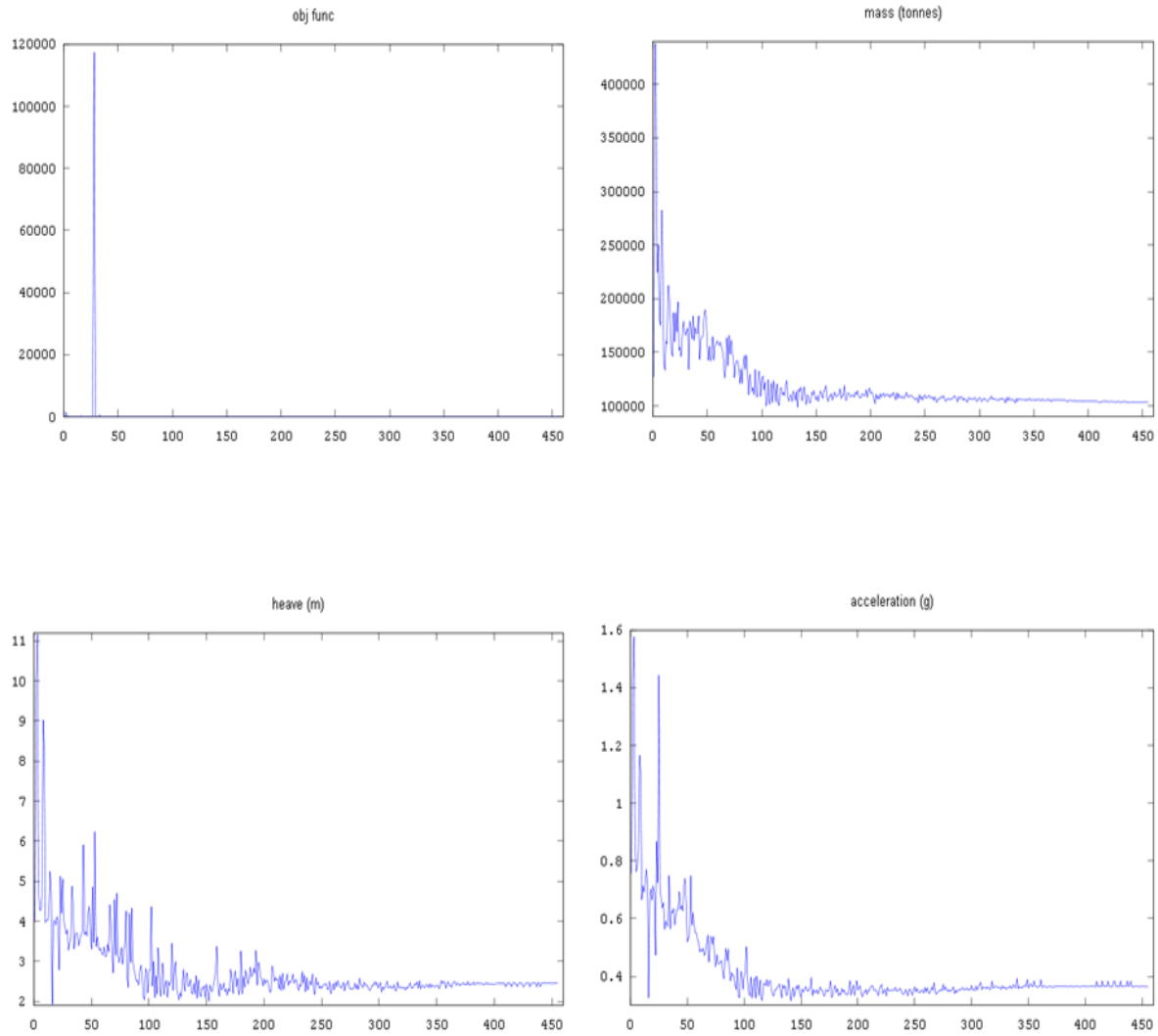

Figure 12.1 Key responses vs. iterations

After optimizing the unit, optimized parameter data are collected and put as input data for analysing the model again with a normal mode. After analysing the model, the following important results are listed below and compared with target values.

Panel models of this non-conventional unit before and after optimization are shown in Figure 12.2. Geometric changes have occurred regarding the dimensions of the pontoon between columns and outside columns and also the dimensions of the columns during the optimization.

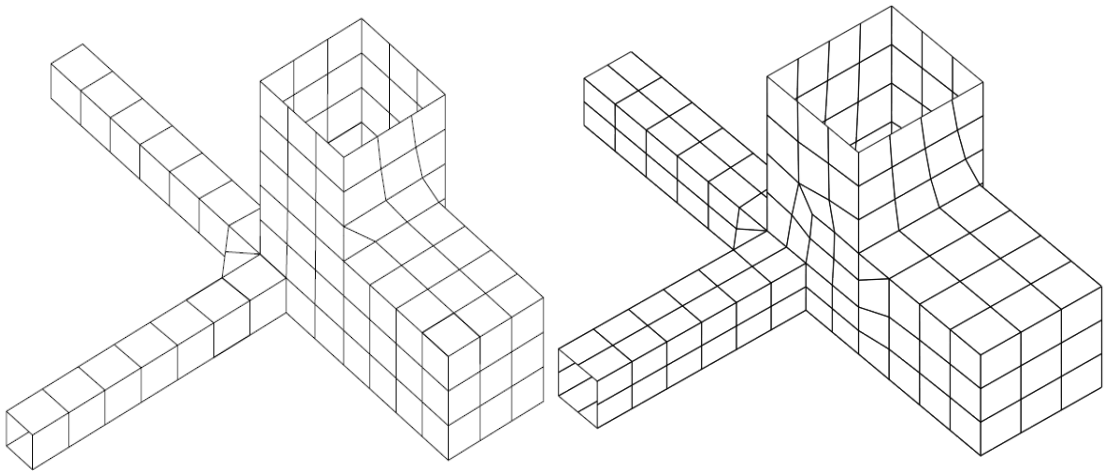

Figure 12.2 Panel model of the non-conventional unit before (left) and after optimization (right)

The most maximum probable value of a heave motion is shown in Table 12.1 and the heave Response Amplitude Operator (RAO) before and after optimization is illustrated in Figures 12.3 and 12.4. For column-stabilized units it is always important that the resonance period is far away from the wave period and the amplitude of the hump should be decreased, since the sea period is normally located in the same region. Comparing the heave motion before and after optimization, the resonance period after optimization moves further to the normal sea period, so the probability that resonance occurs will be reduced. This is one of the two significant improvements for the optimization. The amplitude of the hump after optimization increases but it is an acceptable value, while in the head direction, the most probable maximum value of the heave motion is reduced. However, in quarter sea and beam sea it increases.

Table 12.1 The most probable maximum value of the heave motion

Wave propagating towards	Heave motion	
	before optimization	after optimization
Bow	2.2 m	1.8 m
Quartering	1.8 m	2.2 m

Beam	3.3 m	3.6 m

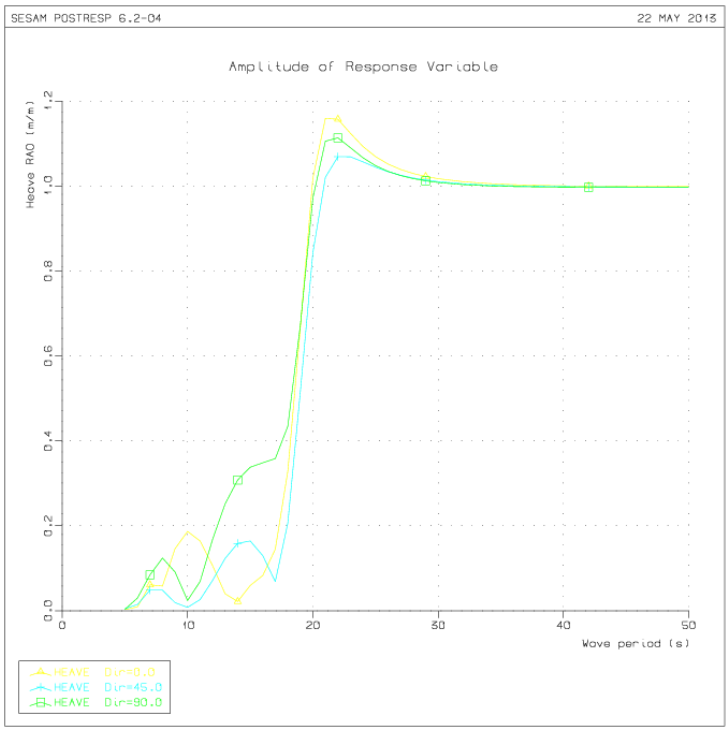

Figure 12.3 Heave RAO of the non-conventional unit before optimization

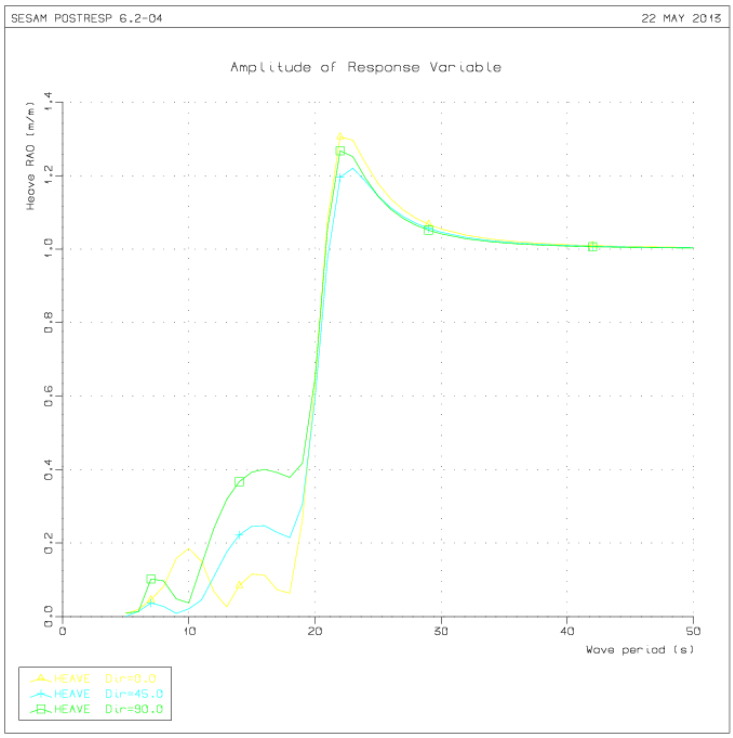

Figure 12.4 Heave RAO of the non-conventional unit after optimization

The comparison between calculation results and target values for this non-conventional unit is listed in Table 12.2. Except for the increase of the eigenperiod another significant improvement is the reduction of width. A dry dock can normally construct a platform with a width of 99 metres but not 112 meters. But there are also problems with air gap and pontoon stress. The pontoon stress shown here is just a rough estimation, but it indicates that structural damage may occur. However, a further detailed structural calculation is necessary in order to check the pontoon strength since it is possible that the stress will be redistributed and the pontoon stress will be reduced. A negative air gap may result in the wave-in-deck force, which will be illustrated in Section 12.4.3.

Table 12.2 Comparison between calculation results and target values for the non-conventional unit

Considered response and geometric limits	Results from analysis model		Target value
	Start guess	Optimized	
Offset amplitude (% of water depth)	6.7	6.5	≤7.0
Heel amplitude (˚)	3.9	4.2	≤5.5
Heave amplitude (m)	3.3	3.6	≤2.0
Metacentric height (m)	13.2	1.6	≥2.0

Air-gap (m)	-7.2	-2.4	≥ 1.5
Acceleration (g)	0.66	0.74	≤ 0.15
Total mass (10^3 tonnes)	59	75	≤ 10
Pontoon stress (MPa)	1825	892	≤ 150
Eigenperiod associated with heave motion (s)	19.8	21.2	≥ 22
Draught (m)	30	30	≤ 30
Width (m)	112	99	≤ 80

It is clear that after optimization there is a great improvement in width reduction and a reasonable improvement in air-gap and eigenperiod. But in the maximum heave amplitude, the improvement even increases in the quarter and beam direction, while it deceases in the head direction. Now it is necessary to make sure that these are values that are improved compared to a traditional conventional unit with the same environmental and geometri conditions. After comparing, it can be concluded that this non-conventional unit can give a better result in a heave motion. Figure 12.5 shows that in quarter sea and beam sea, the amplitude of the hump is reduced significantly. The most maximum probable value of the heave motion is shown in Table 12.3.

Table 12.3 Most probable maximum value of the heave motion

Wave propagating towards	Heave motion	
	Traditional unit	Non-conventional unit
Bow	4.7 m	1.8 m
Quartering	4.6 m	2.2 m
Beam	4.7 m	3.6 m

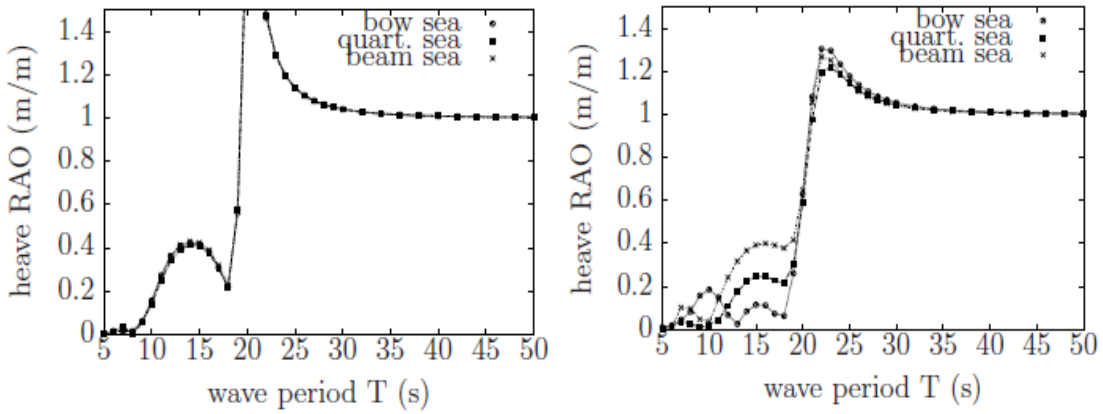

Figure 12.5 Heave RAO of the Traditional unit (left) and an optimized non-conventional unit (right)

12.4 A detailed analysis of the non-conventional unit

Regarding the computational result in Section 12.3, a detailed analysis on the heave motion, stability, air gap , structural analysis of the pontoon extensions and mooring stiffness and capacity of the optimized non-conventional unit is shown in this section.

12.4.1 Heave motion

The heave motion of a semi-submersible in beam seas can be formulated as (cf. Faltinsen (1993)):

$$\frac{\eta_3}{\varsigma_a} = \sin \omega t e^{kz_m} \cos(kB/2) \left(1 - \frac{kz_m}{1 - \left(\frac{\omega}{\omega_n} \right)} \right) \tag{12.1}$$

where

$$\omega_n = \left(\frac{\rho g A_w}{M + A_{33}} \right)^{1/2} \tag{12.2}$$

In Equations (12.1) and (12.2), ω is the frequency of the wave, η_3 is the heave elevation, M is the mass of the platform, A_{33} is the added mass coefficient, A_w is the water plane area of the semi-submersible, ς_a is the wave amplitude, k is the wave number and B is the distance between the centre planes of each pontoon.

Equation (12.2) is the natural circular frequency in heave. When $\omega_n = \omega$, which means that the natural frequency is equal to the wave frequency, the heave motion is infinite and resonance appears. But this is not realistic since the viscous damping

effect is neglected. In reality, it is shown as in Figures 12.3 and 12.4 that when the wave period is close to the eigenperiod, the heave amplitude becomes very large.

The heave motion can be considered the resultant of two principal components. The first component is the response to the oscillatory forces exerted by the wave on the columns. The second component is the response to the oscillatory forces acting on the pontoons. For a non-conventional unit, the force on the pontoon can be partially cancelled due to the outboard extension. This will be shown in the following:

Assume that a wave passes through a semi-submersible and the wave crest appears at the centre of the platform. Based on potential theory and the Bernoulli equation, the dynamic pressure induced by waves can be derived as:

$$p = \rho g a e^{kz} \cos(kx - wt) - \rho g z \tag{12.3}$$

From Equation (12.3) it can be seen that a wave crest gives a higher pressure. That is why, in a semi-submersible, different part of the pontoons contribute unequally to the total dynamic pontoon force when analysed with respect to a wave crest appearing at the centre of the semi-submersible. In particular, the inboard portions contribute more dynamic force per volume because they are at the wave crest while the outboard portions contribute less dynamic force per volume because they are located near the wave troughs.

But as described in Section 5.3, there is an outboard extension with a suitable length for the non-conventional unit, which can partially but not totally cancel the dynamic force on the pontoon. Consequently, in the presence of a wave crest, the total dynamic force on both pontoon and column can be reduced, thereby reducing the heave motion. If the length of the outboard extension is not appropriate, a possible result is that it will totally cancel the dynamic force on the pontoon and thus the force on the column will be dominant, which is unexpected.

12.4.2 Stability

For operational conditions, the metacentric height before optimization is $GM_l = 13.2$ m and $GM_t = 13.2$ m in the longitudinal and transverse direction, respectively. But the metacentric height for the optimized platform is $GM_t = 1.6$ m and $GM_l = 2.86$ m, which decreases significantly. This is mainly due to the shift of the centre of gravity. The metacentric height after optimization is slightly low for a robust design and further investigation could be made to increase it.

12.4.3 Air gap

A positive air gap should generally be ensured including the relative motion of the platform and interaction effects (cf. DNV (2008)). A negative air gap may be considered as being acceptable for overhanging structures and appendages to the deck structure. The response spectrum of the relative motion r is calculated as follows:

$$r(\omega) = 1.2e(\omega) - z(\omega) \tag{12.4}$$

Where ω denotes the angular frequency, e denotes the wave crest and z denotes the absolute motion of the studied location. Moreover, the purpose of the factor 1.2 in Equation (12.4) is to account for deviations from an ideal sinusoidal wave for semi-submersibles or TLP (cf. DNV (2010)). The most probable maximum $X(r)$ is calculated from the spectrum $r(\omega)$, whereby the most probable minimum air gap is calculated by subtracting $X(r)$ from the static air gap .

The target value of the most probable minimum air gap is set to 1.5 m considering operational aspects and requirements for inspection and maintenance. But the air gap for an optimized value is -2.4 m. This negative value may result in the wave impact on deck and this wave impact should be taken into fully account in the structural design and it may lead to structural failure.

12.4.4 Structural analysis of pontoon extensions

In Figure 12.2 it is seen that the optimization result gives wide but short pontoon extensions, which may cause problems in structure strength. Thus, in this section, a rough evaluation with respect to shear strength of the extensions is shown below.

The sea pressures attacking the extensions can be estimated as (cf. DNV (2008)):

$$p \approx \rho g z + \rho g a e^{-2\pi z/\lambda} = 370 \text{ kPa} \tag{12.5}$$

where draught $z = 30\,\text{m}$, $a = H_s = 14\,\text{m}$, $\lambda_s = 321\,\text{m}$. The first term in Equation (12.5) is static pressure and the second term is dynamic wave pressure. The shear force can be obtained by integrating pressure in the upper surface of the extension:

$$V = \int_{\Omega} p ds \approx pS = 146 \text{ MN} \tag{12.6}$$

where S is the upper surface of the extension, and can be calculated by:

$$S = s_{13} \times s_{14} = 396 \text{ m}^2 \tag{12.7}$$

s_{13} and s_{14} are defined in Appendix 2.

The side plating and the interior bulkhead is exposed to shearing due to loading V. The shear stress in the bulkhead is estimated as:

$$\tau \approx \frac{V}{12ht} = 68 \text{ MPa} \tag{12.8}$$

where $h = 15$ m and $t = 12$ mm, the minimum thickness of the plating.

The design yield strength $f_{yd} = 308$ MPa corresponding to a high-strength steel NV-36 is assumed. Then the safety margin for shear strength is $\tau_{yd} = f_{yd} / \sqrt{3} = 177$ MPa. The safety factor $s = \tau_{yd} / \tau - 1 = 1.6$.

12.4.5 Mooring stiffness and capacity

Mooring stiffness depends on pre-tension , the mass of mooring line, type of rope, water depth and spreading. The stiffness of a spread mooring system is considered in surge, sway, yaw and the equations of the stiffness are described in Equations (10.31), (10.32) and (10.33). Results of mooring stiffness in different components are shown in Table 12.4.

Table 12.4 Mooring stiffness of the non-conventional unit

Component	Stiffness
surge-surge	C_{11} =99 kN/m
sway-sway	C_{22} =99 kN/m
yaw-yaw	C_{66} =2996 MNm/radians

The mooring capacity is presented in terms of factors of safety, and the factors of safety are defined as a ratio of break load and maximum line tension. To calculate the static offset, it is assumed that the wind direction and current direction coincide and the static offset is calculated from the following formula:

$$staticoffset = \frac{\sqrt{surge^2 + sway^2}}{waterdepth} \times 100\% \tag{12.9}$$

The target value of the static offset is lower than 7% and the safety factor is greater than 2.7. In this analysis, the static offset in the bow and beam direction fulfil the target value as shown in Table 12.5, while the safety factor of the lines are presented in Table 12.6, and the safety factor for all mooring lines in all directions also fulfil the target value.

Table 12.5 Static offset of the non-conventional unit

Wind and current propagating towards	Surge (m)	Sway (m)	$\frac{\sqrt{surge^2 + sway^2}}{waterdepth} \times 100\ \%$
Bow	32	0	6.5
Quartering	25	25	7.2
Beam	0	32	6.5

Table 12.6 Safety factor of mooring lines for the non-conventional unit

Mooring line	Wind and current direction		
	bow	quartering	beam
1	13.2	46.9	13.2
2	13.2	46.9	13.2
3	13.2	46.9	13.2
4	13.2	46.9	13.2
5	3.7	5.8	13.2
6	3.7	5.8	13.2
7	3.7	5.8	13.2
8	3.7	5.8	13.2
9	3.7	3.1	3.7
10	3.7	3.1	3.7
11	3.7	3.1	3.7
12	3.7	3.1	3.7
13	13.2	5.8	3.7
14	13.2	5.8	3.7
15	13.2	5.8	3.7
16	13.2	5.8	3.7

13 Concluding Remarks

HYDA is a powerful tool and can perform state-of-the-art analysis for thye design and optimization of different types of floating platforms. As clarified in the objective, there are two parts in the project: modification of software HYDA and optimization of the non-conventional unit.

For the first part of the project, after modification one more reference model is taken into consideration and piecewise functions are adopted in order to give a more accurate estimation for mass budget scaling. The superstructure and area of facilities on deck are included in the projected area of platforms for wind-force scaling. Moreover, similar to mass budget scaling, one more reference model is introduced and piecewise functions are adopted in wind-force scaling. Current force scaling for a sway and roll response is modified, while for surge and pitch it is kept unchanged. In the mooring stiffness calculation the number of possible mooring angle combinations is increased and the mean wave-drift force is included in the static offset calculation. So for this part the goal has been reached.

For the second part, the optimization of a non-conventional unit is assessed using HYDA, and the motion response before and after optimization is compared and analysed. From the comparison it is concluded that the width of the platform after optimization is significantly reduced while the eigenperiod increases. Both of the non-conventional units before and after optimization give a good result in the heave motion - considerably reduced compared to a conventional unit. But problems appear with air gap and pontoon stress. A negative air gap appears and a high pontoon stress may result in structure damage. So, the goal of this second part has not been fully realized because the optimization procedure is complicated and depends on several weighting factors. Further investigation is necessary on the optimization of a non-conventional unit in order to achieve a platform with good performance in all the considered responses.

14 References

G. Bergman (1978): *Heave stabilization of semi-submersible platforms*. United States patent, 4112864, Montecito, California, 63-65 pp.

O. M. Faltinsen (1993): *Sea loads on ships and offshore structures*. Cambridge University Press, Cambridge.

DNV (2008): *Structural design of column stabilized units* (LRFD method), Sec.4, DET NORSKE VERITAS AS, DNV-OS-C103, Oslo, Norway, 17 pp.

DNV (2010): *Environmental conditions and environmental loads*, Sec.4, DET NORSKE VERITAS AS, DNV-RP-C205, Oslo, Norway, 76-77 pp.

Journee, J.M.J. and Massie, W.W. (2001): *Offshore hydromechanics*, Delft University of Technology, Delft, Netherland.

DNV (2010): *Global performance analysis of deepwater floating structures*, DET NORSKE VERITAS AS, DNV-RP-F205, Oslo, Norway, 8-9 pp.

NORSOK (2010): *Actions and action effects*, Standard Norway, NORSOK STANDARD N-003, Oslo, Norway, 45-46 pp.

MARINTEK (2010): *MIMOSA 6.3-User's Documentation*, Norwegian Marine Technology Research Institute, Trondheim, Norway, 22-23 pp.

DNV (2010): *Position mooring*, Sec.4. DET NORSKE VERITAS AS, DNV-OS-E103, Oslo, Norway, 29-31 pp.

API (2005): *Design and analysis of stationkeeping systems for floating structures*, American Petroleum Institute, Washington, American, 15-18 pp.

DNV (2007): *SESAM User Manual POSTRESP*, DET NORSKE VERITAS AS, Oslo, Norway.

DNV (2008): *SESAM User Manual WADAM*, DET NORSKE VERITAS AS, Oslo, Norway.

Appendix 1: Revision and Update History of HYDA

- Program package: HYDA
  Created by: GJ January 2011
  Purpose to create: aid in design of floating production platforms
  Purpose to modify: refine some of the subroutines with regard to mass budget, wind-force scaling, current force scaling, mooring systems and static offset.
  Modified by: Hao and Mezbah April 2013

- Subroutines: DEFAULTPARAM and READINPUTFILE
  Purpose to create: set start parameter values
  Created by: GJ January 2011
  Purpose to modify: make the subroutine correspond to modified input file
  Modified by: Hao and Mezbah April 2013
  Called by: main program HYDA

- Subroutine: MASSBUDGET
  Purpose to create: estimate mass budget
  Created by: GJ January 2011
  Called by: main program HYDA
  Overall check of semi equipment list by: GJ 10 August 2011
  Purpose to modify: introduce a flag to define a reference model (predefined or user-defined)
  Modified by: Hao and Mezbah April 2013

- Subroutine: EQUIPMENTLIST1
  Purpose to create: scale mass budget for model type 1
  Created by: GJ January 2011
  Called by: Subroutine MASSBUDGET
  Purpose to modify: introduce two reference models to estimate the mass budget
  Modified by: Hao and Mezbah April 2013

- Subroutine: EQUIPMENTLIST3
  Purpose to create: scale mass budget for model type 3
  Created by: GJ January 2011
  Called by: Subroutine MASSBUDGET

- Subroutine: EQUIPMENTLIST4
  Purpose to create: scale mass budget for model type 4
  Created by: GJ January 2011
  Called by: Subroutine MASSBUDGET

- Subroutine: EQUIPMENTLIST5
  Purpose to create: scale mass budget for model type 5
  Created by: GJ January 2011

Called by: Subroutine MASSBUDGET

- Subroutine: EQUIPMENTLIST9
  Purpose to create: scale mass budget for model type 9
  Created by: GJ January 2011
  Called by: Subroutine MASSBUDGET

- Subroutine: EQUIPMENTLIST12
  Purpose to create: scale mass budget for model type 12
  Created by: GJ January 2011
  Called by: Subroutine MASSBUDGET

- Subroutine: MASSCALCULATION
  Purpose to create: calculate total mass and radii of gyration
  Created by: GJ January 2011
  Called by: Subroutine MASSBUDGET

- Subroutine: PGENIE
  Purpose to create: create panel model
  Created by: GJ Mars 2011
  Called by: main program HYDA

- Subroutine: PGENIE1
  Purpose to create: generate model type 1
  Created by: GJ Mars 2011
  Called by: Subroutine PGENIE

- Subroutine: PGENIE2
  Purpose to create: generate model type 2
  Created by: GJ Mars 2011
  Called by: Subroutine PGENIE

- Subroutine: PGENIE3
  Purpose to create: generate model type 3
  Created by: GJ Mars 2011
  Called by: Subroutine PGENIE

- Subroutine: PGENIE4
  Purpose to create: generate model type 4
  Created by: GJ Mars 2011
  Called by: Subroutine PGENIE

- Subroutine: PGENIE5
  Purpose to create: generate model type 5
  Created by: GJ Mars 2011
  Called by: Subroutine PGENIE

- Subroutine: PGENIE6
  Purpose to create: generate model type 6
  Created by: GJ Mars 2011

Called by: Subroutine PGENIE

- Subroutine: PGENIE7
  Purpose to create: generate model type 7
  Created by: GJ Mars 2011
  Called by: Subroutine PGENIE

- Subroutine: PGENIE8
  Purpose to create: generate model type 8
  Created by: GJ Mars 2011
  Called by: Subroutine PGENIE

- Subroutine: PGENIE9
  Purpose to create: generate model type 9
  Created by: GJ Mars 2011
  Called by: Subroutine PGENIE

- Subroutine: PGENIE10
  Purpose to create: generate model type 10
  Created by: GJ Mars 2011
  Called by: Subroutine PGENIE

- Subroutine: PGENIE11
  Purpose to create: generate model type 11
  Created by: GJ Mars 2011
  Called by: Subroutine PGENIE

- Subroutine: PGENIE12
  Purpose to create: generate model type 12
  Created by: GJ Mars 2011
  Called by: Subroutine PGENIE

- Subroutine: PGENIE13
  Purpose to create: generate model type 13
  Created by: GJ Mars 2011
  Called by: Subroutine PGENIE

- Subroutine: PGENIE14
  Purpose to create: generate model type 14
  Created by: GJ Mars 2011
  Called by: Subroutine PGENIE

- Subroutine MORISON
  Purpose to create: create slender element model
  Created by: GJ Mars 2011
  Called by: main program HYDA

- Subroutine CATMOOR
  Purpose to create: calculate catenary mooring stiffness
  Created by: GJ 15 Mars 2011

Purpose to modify: change the angle combination of mooring lines
Modified by: Hao and Mezbah April 2013
Called by: main program HYDA

- Subroutine STATICOFFSET
  Purpose to create: calculating static offset
  Created by: GJ Mars 2011
  Purpose to modify: introduce environment load in an accurate way
  Modified by: Hao and Mezbah April 2013
  Called by: main program HYDA

- Subroutine PREFEM
  Purpose to create: generation of post-script figures
  Created by: GJ Mars 2011
  Called by: main program HYDA

- Subroutine: WINDFORCE
  Purpose to create: estimate wind-force coefficients
  Created by: GJ April 2011
  Called by: main program HYDA
  Overall check by: GJ August 2011
  Comparative check by: GJ August 2011
  Purpose to modify: introduce experiment data from wind tunnel;
  consider the above area of platforms, which may have an effect on wind resistance
  Modified by: Hao and Mezbah April 2013

- Subroutine: CURRFORCE
  Purpose to create: estimate current force coefficients
  Created by: GJ April 2011
  Called by: main program HYDA
  Overall check by: GJ August 2011
  Comparative check by: GJ August 2011
  Purpose to modify: modify the typical dimensions of the platforms used in the formula for estimating current resistance
  Modified by: Hao and Mezbah April 2013

- Subroutine: OBJECTFUNC
  Purpose: calculate object function to minimize
  Created by: GJ April 2011
  Called by: main program HYDA
  Overall check by: GJ August 2011

- Subroutine CHECKPARAM
  Purpose: check for conflicts between parameters
  Created by: GJ May 2011
  Called by: main program HYDA

- Subroutine STRUCPONTOON
  Purpose: assess strength of pontoon

Created by: GJ May 2011
Called by: main program HYDA

- Subroutine CASH
  Purpose: calculate non-linear and low-frequent responses
  Created by: GJ May 2011
  Called by: main program HYDA
  Calls: external program CASH

- Subroutine GM
  Purpose: calculate GZ-curve
  Created by: GJ June 2012
  Called by: main program HYDA
  Calls: external program READLIS

- Subroutine READWADAMLIS
  Purpose: read basis properties from WADAM result list
  Created by: GJ June 2012
  Called by: main subroutine GM among others

- Subroutine MEANDRIFT
  Purpose to create: calculate mean drift force and calculate the static offset again including the mean drift force
  Created by: Hao and Mezbah April 2013
  Called by: main program HYDA

Appendix 2: Geometry Types in HYDA

The appendix presents the geometry types implemented in the tool HYDA. Some of them are used in Chapter 5 and Chapter 12.

1. (4S) 4 legs outside square ring pontoon:

   This geometry resembles a double symmetric production platform of the JSM type. The main geometric parameters are illustrated below. The following geometry inputs are required for this geometry type:

   - Length over columns
   - Length over pontoons
   - Height of pontoons
   - Keel to box bottom
   - Column side
   - Column radius
   - Bilge radius
   - Draught
   - Cakepiece

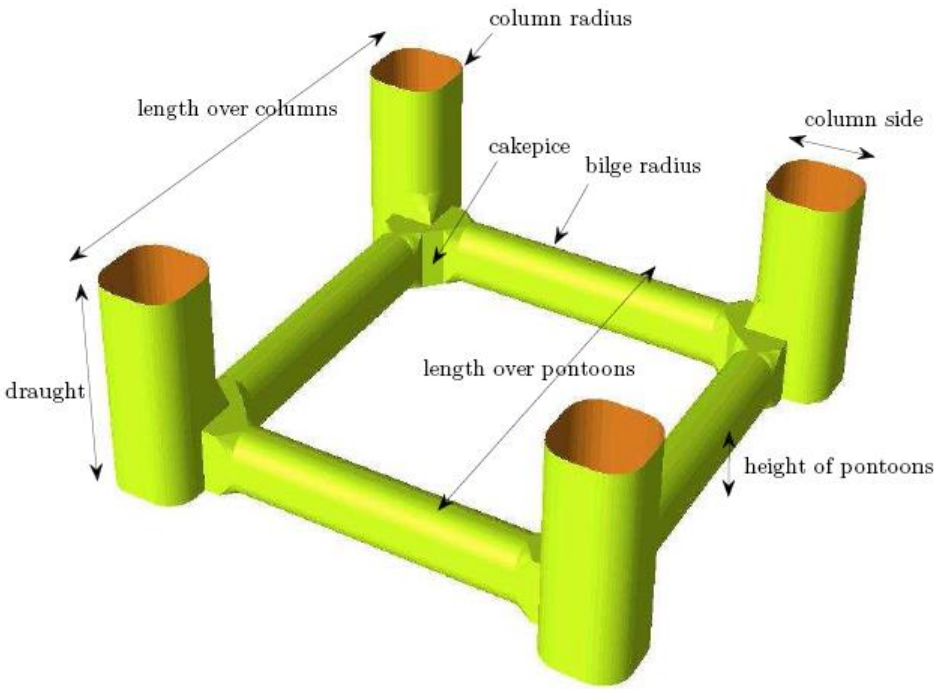

Figure A2.1 4S platform and its geometric parameters

2. (4R) 4 legs outside rectangular ring pontoon

This geometry is a generalization of (4S), such that the length and the width can be different. The reference model of the production unit analysed in Chapter 5 is this type. The main geometric parameters are illustrated below and the following geometry inputs are required for the geometry type. The figures in brackets are the input data used in the reference model in Chapter 4.

- Length over columns (116. m)
- Length over pontoons (105. m)
- Height of pontoons (11.5 m)
- Keel to box bottom (61.5 m)
- Column side (23. m)
- Column radius (5. m)
- Bilge radius (1.3 m)
- Draught (41.5 m)
- Cakepiece (7.05 m)
- Width over columns (115. m)

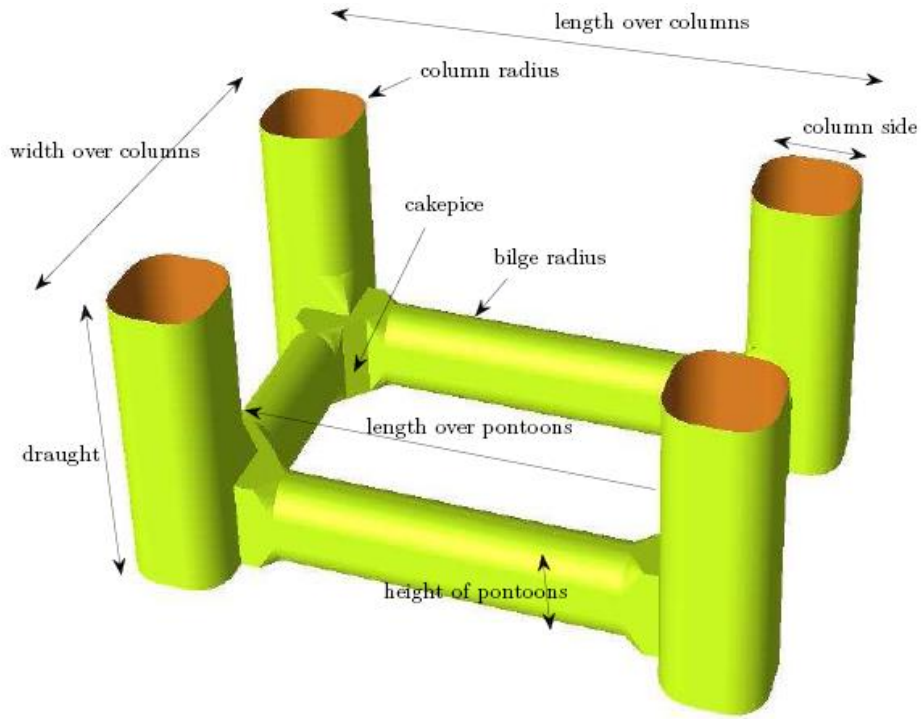

Figure A2.2 4R platform and its geometric parameters

The primary input used in the reference model of the production unit in Chapter 5 is listed below:

- Topside mass (28444 tonnes)
- Riser mass (10707 tonnes)
- Umbilical mass (2460 tonnes)
- Water depth (2130 m)
- Significant wave height (14.70 m)
- Min peak period (11.00 s)
- Max peak period (14.80 s)
- Wind velocity, one hour average at 10 m altitude (39.0 m/s)
- Surface current (1.58 m/s)
- Number of equally spread mooring lines (16)

3. (S4) Square ring pontoon under 4 circular legs

This double symmetric geometry is similar to (4S). The main geometric parameters are illustrated below and the following geometry inputs are required for this geometry type:

- Length over columns
- Height of pontoons
- Keel to box bottom
- Column side
- Draught
- Cakepiece

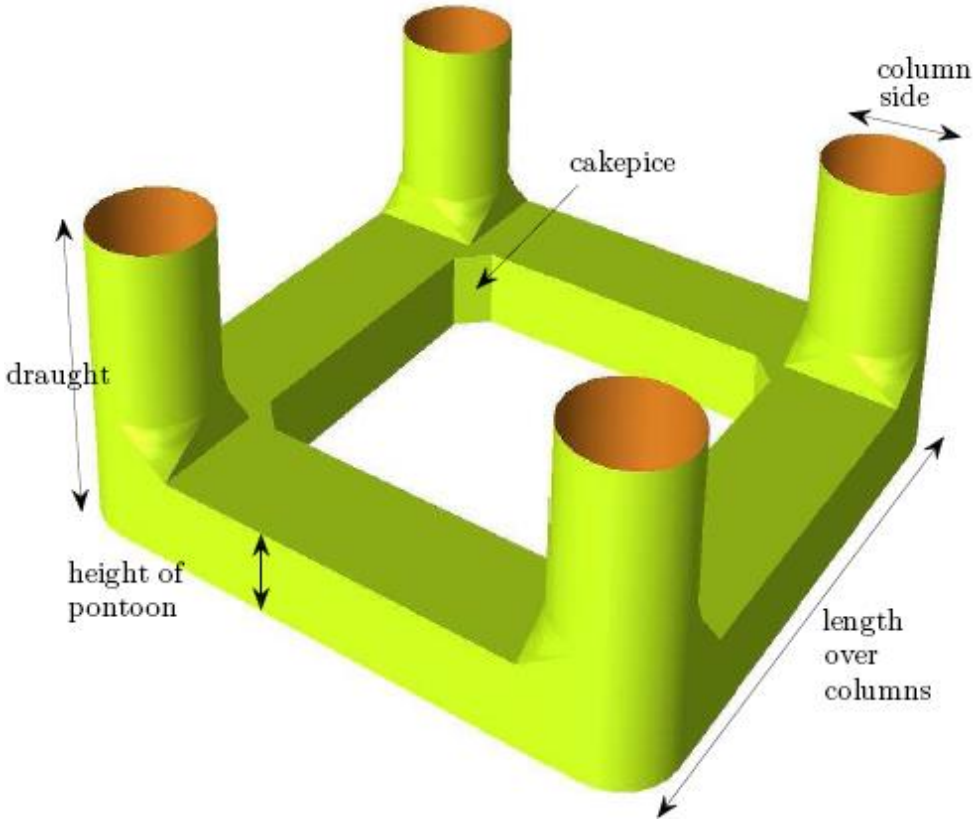

Figure A2.3 S4 platform and its geometric parameters

4. (R4) Rectangular ring pontoon under 4 circular legs

This geometry is a generalization of (S4), such that the length and width can be different. The main geometric parameters are illustrated in the figure below. The following geometry inputs are required for this geometry type:

- Length over columns
- Height of pontoons
- Keel to box bottom
- Column side
- Draught
- Cakepiece
- Width over columns

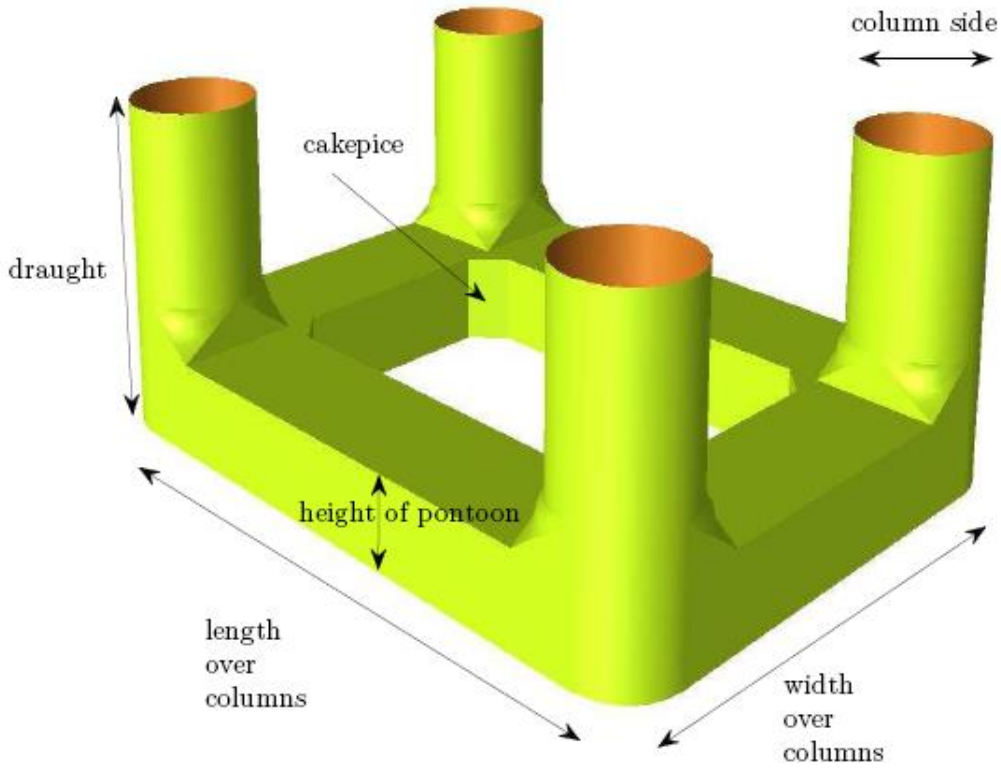

Figure A2.4 R4 platform and its geometric parameters

5. (D4) Drilling unit with 4 legs

The reference model of the drilling unit analysed in Chapter 5 is this type. The main geometric parameters are illustrated below and the following geometry inputs are required for the geometry type. The figures in brackets are the input data used in the reference model in Chapter 5.

- Length over pontoons (89.68 m)
- Height of pontoons (9.10 m)
- Keel to box bottom (35.90 m)
- Column side (13.68 m)
- Column radius (5. m)
- Draught (25.00 m)
- Width over columns (70.72 m)
- Longitudinal x. position of columns (28.12 m)
- Longitudinal x. distance over front deck (0.5 m)
- Excess width of pontoon as compared to column side (2.32 m)
- Width of wing (10. m)
- Longitudinal x. position of wing (28.12)
- Wing height (3. m)
- Keel to wing-pontoon bottom (3. m)

The primary input used in reference model of drilling unit in Chapter 4 is listed below:

- Topside mass (1000 tonnes)
- Riser mass (1707 tonnes)
- Umbilical mass (20 tonnes)
- Water depth (500 m)
- Significant wave height (13.40 m)
- Min peak period (11.5 s)
- Max peak period (15.00 s)

- Wind velocity, one hour average at 10 m altitude (26.67 m/s)
- Surface current (0.63 m/s)
- Number of equally spread mooring lines (16)

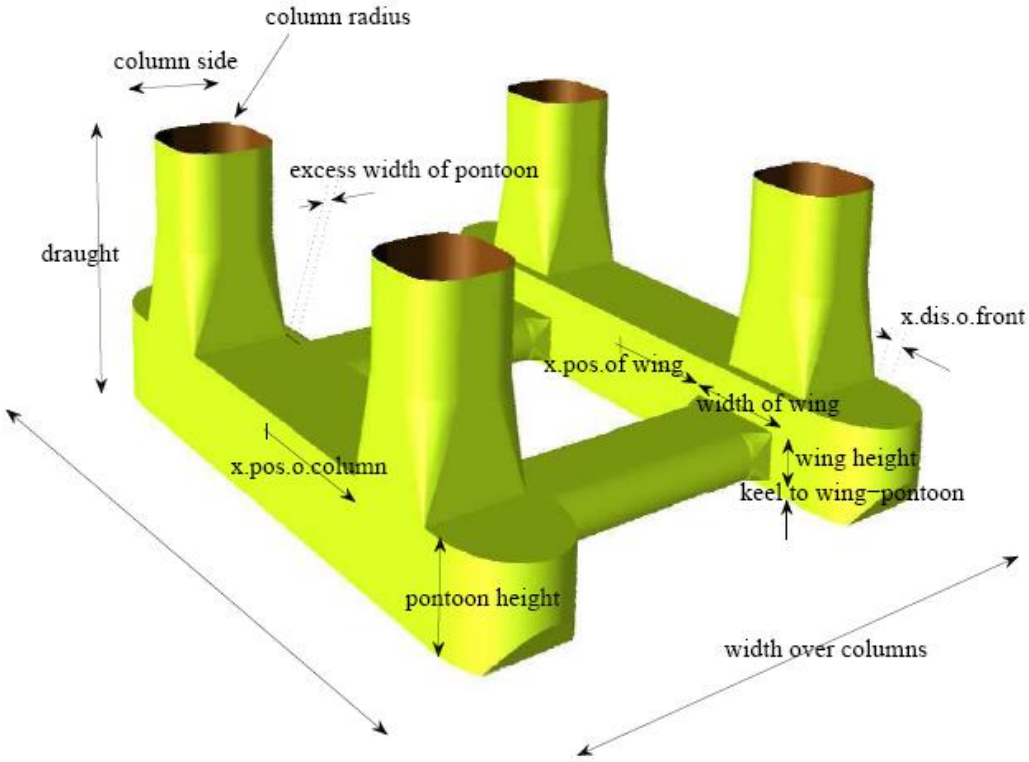

Figure A2.4 D4 platform and its geometric parameters

6. (U2) ugly production unit with 4 legs and box appendices

The U2 type is adopted in the reference model of the non-conventional unit in Chapter 5. The following geometry inputs are required for this type of geometry:

- Longitudinal x. position of wing (47.5 m)
- Pontoon height (13. m)
- Length over pontoons (95. m)
- Pontoon width (11. m)
- Width of wing (11. m)
- Cakepiece side (2. m)
- Column side (21.m)
- 2nd column side (21. m)
- Draught (38. m)
- Front height (25. m)
- X. displacement of front (15. m)
- Front width (10. m)
- Keel to box bottom (63. m)

The primary input used in reference model of non-conventional unit in Chapter 4 is listed below:

- Topside mass (33000 tonnes)
- Water depth (2130 m)
- Significant wave height (14.7 m)
- Min peak period (11. s)
- Max peak period (14.80 s)
- Wind velocity, one hour average at 10 m altitude (39.0 m/s)
- Surface current (1.58 m/s)
- Number of equally spread mooring lines (16)

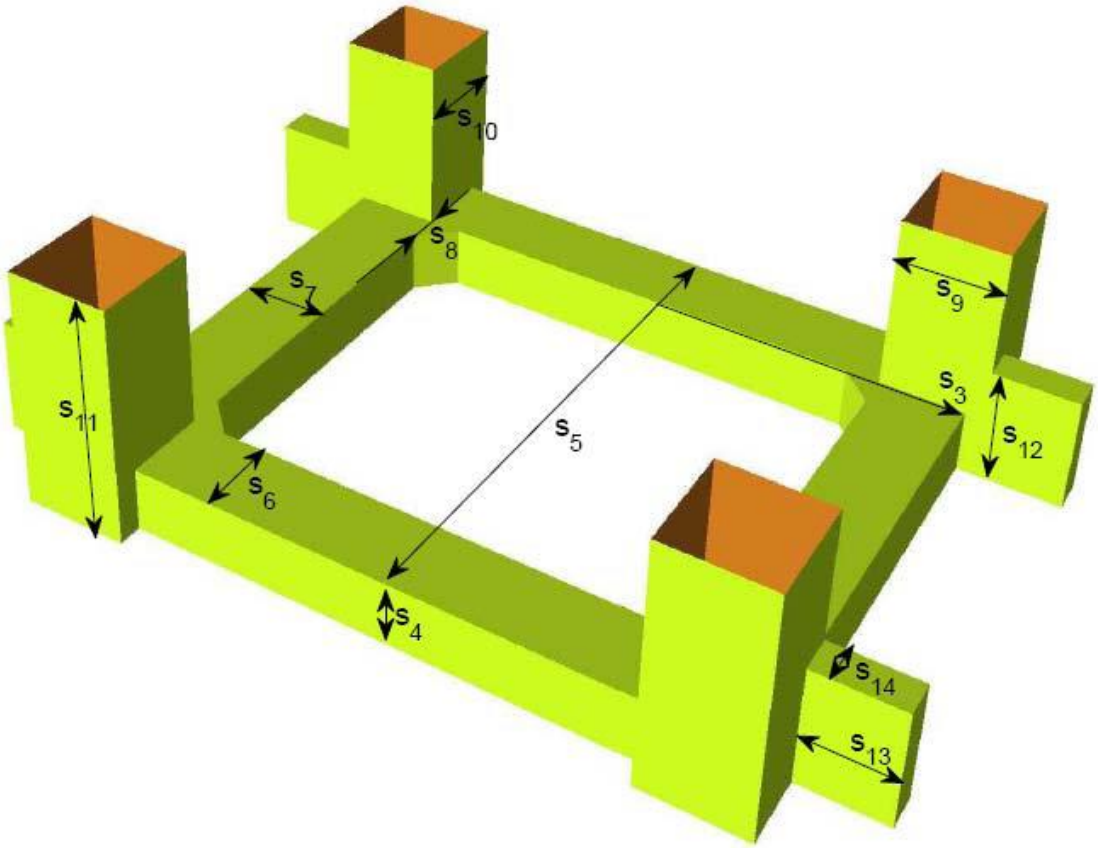

Figure A2.5 U2 platform and its geometric parameters

Appendix 3: Existing Mass Budget Scaling

Item of the floating platform	Mass scaling
Topside	Directly input data
Risers bow	$R/4$
Risers stern	$R/4$
Risers starboard	$R/4$
Risers port side	$R/4$
Equipment	$80\times T/33000$
Umbilical	Directly input data
Management reserve	$0.1862\times T$
Ballast pontoon	Directly input data
Ballast column	0
Fuil oil	$2174\times D/41.5$
Portable water	$1087\times D/41.5$
Bow starboard	$1927\times T/33000$
Bow port	$1927\times T/33000$
Stern port side	$1927\times T/33000$
Stern starboard	$1927\times T/33000$
Pontoon bow	$3560\times W_p\times H_p\times W_{ps}/(105\times 11.5\times 18.5)$
Pontoon stern	$3560\times W_p\times H_p\times W_{ps}/(105\times 11.5\times 18.5)$
Pontoon starboard	$3560\times W_p\times H_p\times W_{ps}/(105\times 11.5\times 18.5)$
Pontoon port side	$3560\times W_p\times H_p\times W_{ps}/(105\times 11.5\times 18.5)$
Column bow starboard	$4100\times D_{ag}\times (L_c)^2/(61.5\times (24.3)^2)$

Column bow port side	$4100 \times D_{ag} \times (L_c)^2 / (61.5 \times (24.3)^2)$
Column stern starboard	$4100 \times D_{ag} \times (L_c)^2 / (61.5 \times (24.3)^2)$
Column stern port side	$4100 \times D_{ag} \times (L_c)^2 / (61.5 \times (24.3)^2)$
Deck box	$13160 \times T / 27000$
Deck house	$2160 \times T / 27000$
Equipment in hull	$500 \times T / 27000$

Appendix 4: Modified Mass Budget Scaling

Item of the floating platform	Mass scaling		
Equipment	$T<T_1$	$T>T_2$	$T_1<T<T_2$
	$E=\frac{(E_1-0)}{(T_1-0)}\times T$	$E=(E_{ul}-E_2)\times(2/\pi)\times\arctan\left(\frac{T}{sT_2}-\frac{1}{s}\right)+E_2$	$E=\frac{(E_2-E_1)}{(T_2-T_1)}\times(T-T_1)+E_1$
Management reserve	$T\times 0.1862$		
Fuil oil	$D<D_1$	$D>D_2$	$D_1<D<D_2$
	$F=\frac{(F_1-0)}{(D_1-0)}\times D$	$F=(F_{ul}-F_2)\times(2/\pi)\times\arctan\left(\frac{D}{sD_2}-\frac{1}{s}\right)+F_2$	$F=\frac{(F_2-F_1)}{(D_2-D_1)}\times(D-D_1)+F_1$
Portable water	$D<D_1$	$D>D_2$	$D_1<D<D_2$
	$P=\frac{(P_1-0)}{(D_1-0)}\times D$	$P=(P_{ul}-P_2)\times(2/\pi)\times\arctan\left(\frac{D}{sD_2}-\frac{1}{s}\right)+P_2$	$P=\frac{(P_2-P_1)}{(D_2-D_1)}\times(D-D_1)+P_1$
Bow starboard	$T<T_1$	$T>T_2$	$T_1<T<T_2$
	$B=\frac{(B_1-0)}{(T_1-0)}\times T$	$B=(B_{ul}-B_2)\times(2/\pi)\times\arctan\left(\frac{T}{sT_2}-\frac{1}{s}\right)+B_2$	$B=\frac{(B_2-B_1)}{(T_2-T_1)}\times(T-T_1)+B_1$
Bow port	$T<T_1$	$T>T_2$	$T_1<T<T_2$
	$B=\frac{(B_1-0)}{(T_1-0)}\times T$	$B=(B_{ul}-B_2)\times(2/\pi)\times\arctan\left(\frac{T}{sT_2}-\frac{1}{s}\right)+B_2$	$B=\frac{(B_2-B_1)}{(T_2-T_1)}\times(T-T_1)+B_1$
Stern port side	$T<T_1$	$T>T_2$	$T_1<T<T_2$
	$B=\frac{(B_1-0)}{(T_1-0)}\times T$	$B=(B_{ul}-B_2)\times(2/\pi)\times\arctan\left(\frac{T}{sT_2}-\frac{1}{s}\right)+B_2$	$B=\frac{(B_2-B_1)}{(T_2-T_1)}\times(T-T_1)+B_1$
Stern	$T<T_1$	$T>T_2$	$T_1<T<T_2$

starboard	$B=\frac{(B_1-0)}{(T_1-0)}\times T$	$B=(B_{ul}-B_2)\times(2/\pi)\times\arctan\left(\frac{T}{sT_2}-\frac{1}{s}\right)+B_2$	$B=\frac{(B_2-B_1)}{(T_2-T_1)}\times(T-T_1)+B_1$
Pontoon bow	$V_a<V_{a1}$	$V_a>V_{a2}$	$V_{a1}<V_a<V_{a2}$
	$M=\frac{(M_1-0)}{(V_{a1}-0)}\times V_a$	$M=(M_{ul}-M_2)\times(2/\pi)\times\arctan\left(\frac{V_a}{sV_{a2}}-\frac{1}{s}\right)+M_2$	$M=\frac{(M_2-M_1)}{(V_{a2}-V_{a1})}\times(V_a-V_{a1})+M_1$
Pontoon stern	$V_a<V_{a1}$	$V_a>V_{a2}$	$V_{a1}<V_a<V_{a2}$
	$M=\frac{(M_1-0)}{(V_{a1}-0)}\times V_a$	$M=(M_{ul}-M_2)\times(2/\pi)\times\arctan\left(\frac{V_a}{sV_{a2}}-\frac{1}{s}\right)+M_2$	$M=\frac{(M_2-M_1)}{(V_{a2}-V_{a1})}\times(V_a-V_{a1})+M_1$
Pontoon starboard	$V_a<V_{a1}$	$V_a>V_{a2}$	$V_{a1}<V_a<V_{a2}$
	$M=\frac{(M_1-0)}{(V_{a1}-0)}\times V_a$	$M=(M_{ul}-M_2)\times(2/\pi)\times\arctan\left(\frac{V_a}{sV_{a2}}-\frac{1}{s}\right)+M_2$	$M=\frac{(M_2-M_1)}{(V_{a2}-V_{a1})}\times(V_a-V_{a1})+M_1$
Pontoon port side	$V_a<V_{a1}$	$V_a>V_{a2}$	$V_{a1}<V_a<V_{a2}$
	$M=\frac{(M_1-0)}{(V_{a1}-0)}\times V_a$	$M=(M_{ul}-M_2)\times(2/\pi)\times\arctan\left(\frac{V_a}{sV_{a2}}-\frac{1}{s}\right)+M_2$	$M=\frac{(M_2-M_1)}{(V_{a2}-V_{a1})}\times(V_a-V_{a1})+M_1$
Column bow starboard	$V_c<V_{c1}$	$V_c>V_{c2}$	$V_{c1}<V_c<V_{c2}$
	$C=\frac{(C_1-0)}{(V_{c1}-0)}\times V_c$	$C=(C_{ul}-C_2)\times(2/\pi)\times\arctan\left(\frac{V_c}{sV_{c2}}-\frac{1}{s}\right)+C_2$	$C=\frac{(C_2-C_1)}{(V_{c2}-V_{c1})}\times(V_c-V_{c1})+C_1$
Column bow port side	$V_c<V_{c1}$	$V_c>V_{c2}$	$V_{c1}<V_c<V_{c2}$
	$C=\frac{(C_1-0)}{(V_{c1}-0)}\times V_c$	$C=(C_{ul}-C_2)\times(2/\pi)\times\arctan\left(\frac{V_c}{sV_{c2}}-\frac{1}{s}\right)+C_2$	$C=\frac{(C_2-C_1)}{(V_{c2}-V_{c1})}\times(V_c-V_{c1})+C_1$
Column stern starboard	$V_c<V_{c1}$	$V_c>V_{c2}$	$V_{c1}<V_c<V_{c2}$
	$C=\frac{(C_1-0)}{(V_{c1}-0)}\times V_c$	$C=(C_{ul}-C_2)\times(2/\pi)\times\arctan\left(\frac{V_c}{sV_{c2}}-\frac{1}{s}\right)+C_2$	$C=\frac{(C_2-C_1)}{(V_{c2}-V_{c1})}\times(V_c-V_{c1})+C_1$
Column	$V_c<V_{c1}$	$V_c>V_{c2}$	$V_{c1}<V_c<V_{c2}$

stern port side	$C=\frac{(C_1-0)}{(V_{c1}-0)}\times V_c$	$C=(C_{ul}-C_2)\times(2/\pi)\times\arctan\left(\frac{V_c}{sV_{c2}}-\frac{1}{s}\right)+C_2$	$C=\frac{(C_2-C_1)}{(V_{c2}-V_{c1})}\times(V_c-V_{c1})+C_1$
Deck box	$T<T_1$	$T>T_2$	$T_1<T<T_2$
	$I=\frac{(I_1-0)}{(T_1-0)}\times T$	$I=(I_{ul}-I_2)\times(2/\pi)\times\arctan\left(\frac{T}{sT_2}-\frac{1}{s}\right)+I_2$	$I=\frac{(I_2-I_1)}{(T_2-T_1)}\times(T-T_1)+I_1$
Deck house	$T<T_1$	$T>T_2$	$T_1<T<T_2$
	$J=\frac{(J_1-0)}{(T_1-0)}\times T$	$J=(J_{ul}-j_2)\times(2/\pi)\times\arctan\left(\frac{T}{sT_2}-\frac{1}{s}\right)+J_2$	$J=\frac{(J_2-J_1)}{(T_2-T_1)}\times(T-T_1)+J_1$
Equipment in hull	$T<T_1$	$T>T_2$	$T_1<T<T_2$
	$K=\frac{(K_1-0)}{(T_1-0)}\times T$	$K=(K_{ul}-K_2)\times(2/\pi)\times\arctan\left(\frac{T}{sT_2}-\frac{1}{s}\right)+K_2$	$K=\frac{(K_2-K_1)}{(T_2-T_1)}\times(T-T_1)+K_1$

Appendix 5: Existing Wind Force Coefficient Scaling

Motion response	Head wind	Quarter wind	Beam wind
Surge force coefficient (kNs^2/m^2)	$4.58 \times W_p \times SAG / (19 \times 105)$	$3.5 \times W_p \times SAG / (19 \times 105)$	0
Pitch moment coefficient (kNs^2/m)	$4.58 \times W_p \times SAG^2 \times 2.04 / (19 \times 105)$	$3.5 \times W_p \times SAG^2 \times 2.04 / (19 \times 105)$	0
Sway force coefficient (kNs^2/m^2)	0	$(3.5 \times W_p \times SAG / (19 \times 105)) \times \frac{L_p}{W_p}$	$(4.58 \times W_p \times SAG / (19 \times 105)) \times \frac{L_p}{W_p}$
Roll moment coefficient (kNs^2/m)	0	$(3.5 \times W_p \times SAG^2 \times 2.04 / (19 \times 105)) \times \frac{L_p}{W_p}$	$(4.58 \times W_p \times SAG^2 \times 2.04 / (19 \times 105)) \times \frac{L_p}{W_p}$

Appendix 6: Modified Wind-Force Coefficient Scaling

Motion response		Head wind	Quarter wind	Beam wind
Surge force coefficient (kNs^2/m^2)	$A_f<A_{f1}$	$H_{su}=\frac{(H_{su1}-0)}{(A_{f1}-0)}\times A_f$	$Q_s=\frac{(Q_{s1}-0)}{(A_{f1}-0)}\times A_f$	0
	$A_f>A_{f2}$	$H_{su}=(H_{sul}-H_{su2})\times(2/\pi)\times\arctan\left(\frac{A_f}{sA_{f2}}-\frac{1}{s}\right)+H_{su2}$	$Q_s=(Q_{sul}-Q_{s2})\times(2/\pi)\times\arctan\left(\frac{A_f}{sA_{f2}}-\frac{1}{s}\right)+Q_{s2}$	0
	$A_{f1}<A_f<A_{f2}$	$H_{su}=\frac{(H_{su2}-H_{su1})}{(A_{f2}-A_{f1})}\times(A_f-A_{f1})+H_{su1}$	$Q_s=\frac{(Q_{s2}-Q_{s1})}{(A_{f2}-A_{f1})}\times(A_f-A_{f1})+Q_{s1}$	0
Pitch moment coefficient (kNs^2/m)	$A_f<A_{f1}$	$H_p=\frac{(H_{su1}-0)}{(A_{f1}-0)}\times A_f\times SAG\times 1.72$	$Q_p=\frac{(Q_{s1}-0)}{(A_{f1}-0)}\times A_f\times SAG\times 1.51$	0
	$A_f>A_{f2}$	$H_p=[(H_{sul}-H_{su2})\times(2/\pi)\times\arctan\left(\frac{A_f}{sA_{f2}}-\frac{1}{s}\right)+H_{su2}]\times SAG\times 1.72$	$Q_p=[(Q_{sul}-Q_{s2})\times(2/\pi)\times\arctan\left(\frac{A_f}{sA_{f2}}-\frac{1}{s}\right)+Q_{s2}]\times SAG\times 1.51$	0
	$A_{f1}<A_f<A_{f2}$	$H_p=[\frac{(H_{su2}-H_{su1})}{(A_{f2}-A_{f1})}\times(A_f-A_{f1})+H_{su1}]\times SAG\times 1.72$	$Q_p=[\frac{(Q_{s2}-Q_{s1})}{(A_{f2}-A_{f1})}\times(A-A_{f1})+Q_{s1}]\times SAG\times 1.51$	0
Sway force coefficient (kNs^2/m^2)	$A_s<A_{s1}$	0	$Q_{sw}=\frac{(Q_{sw1}-0)}{(A_{s1}-0)}\times A_s$	$B_{sw}=\frac{(H_{sw1}-0)}{(A_{s1}-0)}\times A_s$
	$A_s>A_{s2}$	0	$Q_{sw}=[(Q_{swul}-Q_{sw2})\times(2/\pi)\times\arctan\left(\frac{A_s}{sA_{s2}}-\frac{1}{s}\right)+Q_{sw2}]$	$B_{sw}=[(H_{swul}-H_{sw2})\times(2/\pi)\times\arctan\left(\frac{A_s}{sA_{s2}}-\frac{1}{s}\right)+H_{sw2}]$
	$A_{s1}<A_s<A_{s2}$	0	$Q_{sw}=[\frac{(Q_{sw2}-Q_{sw1})}{(A_{s2}-A_{s1})}\times(A_s-A_{s1})+Q_{sw1}]$	$B_{sw}=[\frac{(H_{sw2}-H_{sw1})}{(A_{s2}-A_{s1})}\times(A_s-A_{s1})+H_{sw1}]$

Roll moment coefficient (kNs^2/m)	$A_s<A_{s1}$	0	$Q_r = \frac{(Q_{sw1}-0)}{(A_{s1}-0)} \times A_s \times SAG \times 1.51$	$B_r = \frac{(H_{sw1}-0)}{(A_{s1}-0)} \times A_s \times SAG \times 1.72$
	$A_s>A_{s2}$	0	$Q_r = [\ (Q_{swul}-Q_{sw2}) \times (2/\pi) \times \arctan\left(\frac{A_s}{sA_{s2}}-\frac{1}{s}\right)+Q_{sw2}\ ] \times SAG \times 1.51$	$B_r = [\ (H_{swul}-H_{sw2}) \times (2/\pi) \times \arctan\left(\frac{A_s}{sA_{s2}}-\frac{1}{s}\right)+H_{sw2}\ ] \times SAG \times 1.72$
	$A_{s1}< A_s<A_{s2}$	0	$Q_r = [\ \frac{(Q_{sw2}-Q_{sw1})}{(A_{s2}-A_{s1})} \times (A_s-A_{s1}) + Q_{sw1}\ ] \times SAG \times 1.51$	$B_r = [\ \frac{(H_{sw2}-H_{sw1})}{(A_{s2}-A_{s1})} \times (A_s-A_{s1}) + H_{sw1}\ ] \times SAG \times 1.72$

Appendix 7: Drag Coefficient C_d on Pontoons and Columns (cf. DNV (2010))

l/d	r/d	C_d
<0.75	<0.0105	2.5
	0.0105-0.053	2.2
	0.053-0.1665	1.9
	>0.1665	1.6
0.75-1.5	<0.0105	2.2
	0.0105-0.094	2.0
	0.094-0.25	1.2
	>0.25	1.0
1.5-4.0	<0.021	1.6
	0.021-0.1045	1.4
	0.1045-0.3335	0.7
	>0.3335	0.4
>4.0	<0.25	0.89
	>0.25	0.29

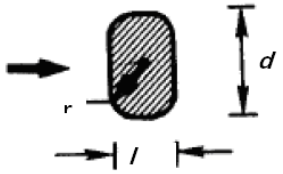

Figure A7.1 Definition of l, r and d for a rectangular with rounded corners

Appendix 8: Existing Current Force Coefficient Scaling

Motion response	Head Current	Quarter current	Beam current
Surge force coefficient (kNs^2/m^2)	$(4\times scol\times D+2\times spon\times W_p)/2$	$(4\times scol\times D+2\times spon\times W_p)/2.4$	0
Pitch moment coefficient (kNs^2/m)	$(4\times scol\times D+2\times spon\times W_p)\times D/(2\times 2)$	$(4\times scol\times D+2\times spon\times W_p)\times D/(2\times 2.4)$	0
Sway force coefficient (kNs^2/m^2)	0	$(4\times scol\times D+2\times spon\times W_p)\times R_p\times L_p/(2.4\times W_p)$	$(4\times scol\times D+2\times spon\times W_p)\times P_p\times L_p/(2\times W_p)$
Roll moment coefficient (kNs^2/m)	0	$(4\times scol\times D+2\times spon\times W_p)\times R_p\times L_p\times D/(2.4\times 2\times W_p)$	$(4\times scol\times D+2\times spon\times W_p)\times R_p\times L_p\times D/(2\times 2\times W_p)$

Appendix 9: Modified Current Force Coefficient Scaling

Motion response	Head Current	Quarter current	Beam current
Surge force coefficient (kNs^2/m^2)	$(4\times scol\times D+2\times spon\times W_p)/2$	$(4\times scol\times D+2\times spon\times W_p)/2.4$	0
Pitch moment coefficient (kNs^2/m)	$(4\times scol\times D+2\times spon\times W_p)\times D/(2\times 2)$	$(4\times scol\times D+2\times spon\times W_p)\times D/(2\times 2.4)$	0
Sway force coefficient (kNs^2/m^2)	0	$(4\times scol\times D+2\times spon\times L_p)\times R_p/2.4$	$(4\times scol\times D+2\times spon\times L_p)\times R_p/2$
Roll moment coefficient (kNs^2/m)	0	$(4\times scol\times D+2\times spon\times L_p)\times R_p\times D/(2.4\times 2)$	$(4\times scol\times D+2\times spon\times L_p)\times R_p\times D/(2\times 2)$

Appendix 10: Derivation for Mean Drift Force in Irregular Waves

Here, a direct-integration method is used to give a brief introduction on the mean drift force since it is straightforward and offers an insight into the mechanism of wave-body interaction (cf. Journee, J.M.J. and Massie, W.W. (2001)).

The derivation is developed using perturbation methods. This indicates that all quantities such as wave height, motions, potentials, and pressures are assumed to vary only slightly relative to the initial value and can be written as:

$$X = X^{(0)} + \varepsilon X^{(1)} + \varepsilon^2 X^{(2)} \tag{A10.1}$$

where $X^{(0)}$ denotes the static value, $X^{(1)}$ denotes the first oscillatory variation and $X^{(2)}$ denotes the second-order variation. The parameter ε is some minor number, with $\varepsilon << 1$, which denotes the order of oscillation. First-order means linearly related to the wave height and second-order means that the quantity depends on the square of the wave height.

The principle of this derivation is to solve governing equations and nonlinear boundary conditions. The complete nonlinear Bernoulli equation is used for deriving the pressure on the body and it assumes that the body is floating in small amplitude waves and only allowed to move in response to first-order hydrodynamic forces at frequencies within the wave frequency region. Thus, here the nonlinear wet surface, nonlinear free surface conditions and nonlinear body boundary conditions are considered.

- **Coordinate system**

Three coordinate systems are used in the derivation, so here a short introduction on coordinate system is given (see figure A10.1):

1. $O-(X_1, X_2, X_3)$ is a right-hand earthbound axes system with the origin O, the X_1- and X_2- axes in the mean free surface of the sea and the X_3-axis positive upwards.

2. $G-(x_1, x_2, x_3)$ is a right-hand system of a body-bound axes system with the centre of gravity as the origin, G, of the body, the positive x_1- axis in the longitudinal direction and the positive x_3- axis upwards. In the mean position of the oscillating vessel, this axes system is parallel to the earthbound system.

3. $G-(X_1^{'}, X_2^{'}, X_3^{'})$ is a moving axes system with its origin in the mean position of the centre of gravity G of the body. Its axes are always parallel to the axes of the earthbound $O-(X_1, X_2, X_3)$ system. So this system does not translate or rotate with the ship's motions.

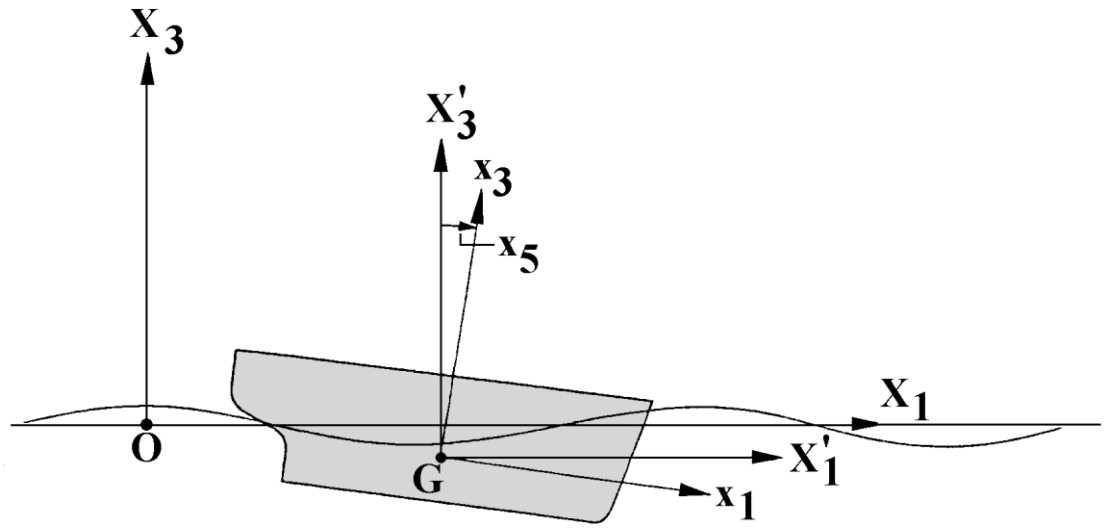

Figure A10.1 System of coordinate axes

- **Body motions**

Assuming that the body has small amplitude motions resulting from the first-order oscillatory wave forces, the resultant displacement vector X can be formulated as:

$$X = \varepsilon X^{(1)} \tag{A10.2}$$

with:

$$X^{(1)} = X_G^{(1)} + R^{(1)} x \tag{A10.3}$$

where $X_G^{(1)}$ is the oscillatory first-order motion vector of the centre of gravity of the body, $x = (x_1, x_2, x_3)$ is the position vector of the point on the body in the bodybound axes system and $R^{(1)}$ is the linearized rotation transformation matrix, defined as:

$$R^{(1)} = \begin{bmatrix} 0 & -x_6^{(1)} & +x_5^{(1)} \\ +x_6^{(1)} & 0 & -x_4^{(1)} \\ -x_5^{(1)} & +x_4^{(1)} & 0 \end{bmatrix} \tag{A10.4}$$

in which $x_4^{(1)}, x_5^{(1)}$, and $x_6^{(1)}$ are the first-order roll, pitch and yaw motions of the structure.

- **Fluid motions**

Assuming that the fluid is inviscid, irrotational, homogeneous and incompressible, the fluid motion can be described by:

$$\Phi = \varepsilon \Phi^{(1)} + \varepsilon^2 \Phi^{(2)} \tag{A10.5}$$

The first-order potential $\Phi^{(1)}$ has already been known as the sum of potentials associated with undisturbed incoming waves, diffracted waves and waves due to the first-order body motions.

- **Continuity equation**

Both the first-order and second-order potentials must satisfy the equation of continuity within the fluid domain:

$$\nabla^2\Phi^{(1)} = 0 \quad \text{and} \quad \nabla^2\Phi^{(2)} = 0 \tag{A10.6}$$

- **Seabed boundary condition**

Both potentials must satisfy the boundary condition at a horizontal seabed

$$\frac{\partial\Phi^{(1)}}{\partial X_3} = 0 \quad \text{and} \quad \frac{\partial\Phi^{(2)}}{\partial X_3} = 0 \tag{A10.7}$$

where $X_3 = -h$, and h is the water depth.

- **Free surface boundary condition**

The free surface condition includes the kinematic and dynamic free surface condition. The kinematic boundary condition states that a particle on the surface will stay at the surface, and the dynamic boundary condition states that the pressure is constant on the free surface condition.

So the homogeneous boundary condition becomes:

$$g\frac{\partial\Phi^{(1)}}{\partial X_3} + \frac{\partial^2\Phi^{(1)}}{\partial t^2} = 0 \tag{A10.8}$$

The particular solution of the boundary condition of $\Phi^{(2)}$ is directly given below without derivation:

$$g\frac{\partial\Phi^{(1)}}{\partial X_3} + \frac{\partial^2\Phi^{(1)}}{\partial t^2} = -2\left(\vec{\nabla}\Phi^{(1)} \cdot \vec{\nabla}\frac{\partial\Phi^{(1)}}{\partial t}\right) + \frac{\partial\Phi^{(1)}}{\partial t}\left(\frac{\partial^2\Phi^{(1)}}{\partial X_3^2} + \frac{1}{g}\cdot\frac{\partial^2}{\partial t^2}\left(\frac{\partial\Phi^{(1)}}{\partial X_3}\right)\right) \tag{A10.9}$$

- **Body surface boundary condition**

In general, the boundary condition on the body is that no fluid passes through the hull. The relative velocity between the fluid and the hull in the direction of the normal to the hull must be zero. This boundary condition has to be satisfied at the instantaneous position of the hull surface, and thus the fluid motions in the direction of the normal on the body have to be equal to the body motion in the normal direction:

$$\vec{\nabla}\Phi \cdot \vec{N} = \vec{V} \cdot \vec{N} \tag{A10.10}$$

- **Pressure acting on the body**

Based on the equations above, the velocity potential can be solved. So the fluid pressure at a point can be determined using a nonlinear Bernoulli equation:

$$p = -\rho g X_3 - \rho \frac{\partial \Phi}{\partial t} - \frac{1}{2}\rho\left(\vec{\nabla}\Phi\right)^2 \tag{A10.11}$$

The point on the hull is carrying out small first-order wave frequency motions $X^{(1)}$, about a mean position, $X^{(0)}$, and the pressure can be expressed as:

$$p = p^{(0)} + \varepsilon p^{(1)} + \varepsilon^2 p^{(2)} \tag{A10.12}$$

where:

- Hydrostatic pressure:

$$p^{(0)} = -\rho g X_3^{(0)} \tag{A10.13}$$

- First-order pressure:

$$p^{(1)} = -\rho g X_3^{(1)} - \rho \frac{\partial \Phi^{(1)}}{\partial t} \tag{A10.14}$$

- Second-order pressure:

$$p^{(2)} = -\frac{1}{2}\rho\left(\vec{\nabla}\Phi^{(1)}\right)^2 - \rho \frac{\partial^2 \Phi^{(2)}}{\partial t^2} - \rho\left(\vec{X}^{(1)} \cdot \vec{\nabla}\frac{\partial \Phi^{(1)}}{\partial t}\right) \tag{A10.15}$$

- **Direct pressure integration**

The drift force F can be obtained by integrating the pressure on the wet surface:

$$F = -\iint_S p\vec{N}dS \tag{A10.16}$$

where S is the instantaneous wetted surface and $\vec{N}$ is the instantaneous normal vector to the surface element dS.

The instantaneous wetted surface can be split into two parts: a constant part S_0 up to the static water line and an oscillating part, s, the splash zone between the static hull waterline and the wave profile along the body.

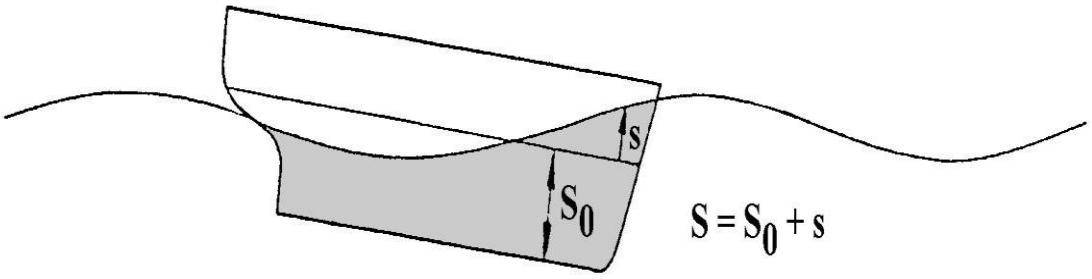

Figure A10.2 Wetted surface of the hull (Journee, J.M.J. and Massie, W.W. (2001))

Substitution of all the terms in Equation (A10.16) yields for the fluid force exerted on the body:

$$F = -\iint_{S_0} \left(p^{(0)} + \varepsilon p^{(1)} + \varepsilon^2 p^{(2)}\right) \cdot \left(\vec{n} + \varepsilon \vec{N}^{(1)}\right) \cdot dS - \iint_{S} \left(p^{(0)} + \varepsilon p^{(1)} + \varepsilon^2 p^{(2)}\right) \cdot \left(\vec{n} + \varepsilon \vec{N}^{(1)}\right) \cdot dS \tag{A10.17}$$

The mean drift force is the time-averaged drift force.

- **Mean drift force in an irregular sea state**

When the results of the mean wave loads in regular waves are known, the results in an irregular sea can be computed. The long crest seas can be described by a PM sea spectrum $S(\omega)$. The mean drift force can be formulated as:

$$\overline{F}_i^s = 2\int_0^\infty S(\omega)\left(\frac{\overline{F}_i(\omega;\beta)}{\zeta_a^2}\right)d\omega \tag{A10.18}$$

where $\overline{F}_i(\omega;\beta)$ is the mean drift force in a regular wave and is calculated based on Equation (A10.17).